

# **Characteristics of Peristaltic Flow of Walters' B Fluid with Chemical Reaction and Convective Conditions**

By

**SYEDA AZKA KHALID**



**NATIONAL UNIVERSITY OF MODERN LANGUAGES**

**ISLAMABAD**

**May, 2024**

# **Characteristics of Peristaltic Flow of Walters' B Fluid with Chemical Reaction and Convective Conditions**

**By**

**SYEDA AZKA KHALID**

National University of Modern Languages, Islamabad, 2024

A THESIS SUBMITTED IN PARTIAL FULFILMENT OF  
THE REQUIREMENTS FOR THE DEGREE OF

**MASTER OF SCIENCE**

**In Mathematics**

To

FACULTY OF ENGINEERING & COMPUTING



NATIONAL UNIVERSITY OF MODERN LANGUAGES ISLAMABAD

© Syeda Azka Khalid, 2024



## THESIS AND DEFENSE APPROVAL FORM

The undersigned certify that they have read the following thesis, examined the defense, are satisfied with overall exam performance, and recommend the thesis to the Faculty of Engineering and Computing for acceptance.

**Thesis Title:** Characteristics of Peristaltic Flow of Walters' B Fluid with Chemical Reaction and Convective Conditions

**Submitted By:** Syeda Azka Khalid

**Registration #:** 26 MS/Math/S21

Master of Science in Mathematics

Title of the Degree

Mathematics

Name of Discipline

Dr. Hadia Tariq

Name of Research Supervisor

\_\_\_\_\_  
Signature of Research Supervisor

Dr. Sadia Riaz

Name of HOD (Mathematics)

\_\_\_\_\_  
Signature of HOD (Mathematics)

Dr. Noman Malik

Name of Dean (FEC)

\_\_\_\_\_  
Signature of Dean (FEC)

May, 2024

## AUTHOR'S DECLARATION

I Syeda Azka Khalid

Daughter of Muhammad Khalid Mehmood

Registration # 26 MS/Math/S21

Discipline Mathematics

Candidate of Master of Science in Mathematics at the National University of Modern Languages do hereby declare that the thesis Characteristics of Peristaltic Flow of Walters' B Fluid with Chemical Reaction and Convective Conditions submitted by me in partial fulfillment of MS Mathematics degree, is my original work, and has not been submitted or published earlier. I also solemnly declare that it shall not, in future, be submitted by me for obtaining any other degree from this or any other university or institution. I also understand that if evidence of plagiarism is found in my thesis/dissertation at any stage, even after the award of a degree, the work may be cancelled and the degree revoked.

---

Signature of Candidate

Syeda Azka Khalid  
Name of Candidate

May, 2024  
Date

## ABSTRACT

### **Title: Characteristics of Peristaltic Flow of Walters' B Fluid with Chemical Reaction and Convective Conditions**

This thesis is primarily focused on examining the peristaltic motion of a Walters' B fluid within an asymmetric porous channel, while also considering chemical reaction and convective boundary conditions. The stream function conversions have been incorporated to the modelled equations to reduce the number of dependent variables. The involvement of the small parameter in the governing equations allow to use perturbation technique to obtain the analytical solution of the problem. The equations have been solved by using Mathematica software. Graphical representations of velocity distribution, temperature profiles, and concentration profiles are studied to provide insights into the interplay of the effect of other parameters within the Walters' B fluid under consideration.

# TABLE OF CONTENTS

CHAPTER	TITLE	PAGE
	<b>AUTHOR'S DECLARATION</b>	iii
	<b>ABSTRACT</b>	iv
	<b>TABLE OF CONTENTS</b>	v
	<b>LIST OF FIGURES</b>	ix
	<b>LIST OF SYMBOLS</b>	xi
	<b>ACKNOWLEDGEMENT</b>	xiii
	<b>DEDICATION</b>	xiv

## Table of Contents

CHAPTER 1.....	2
INTRODUCTION.....	2
1.1 Statics .....	2
1.2 Kinematics.....	2
1.3 Dynamics .....	3
1.4 Steady and Unsteady Fluid .....	3
1.5 Compressible and Incompressible Fluid.....	4
1.6 Viscose or Non-Viscous Fluid .....	4
1.7 Rotational or Irrotational Fluid .....	4
1.8 Ideal Fluid.....	5
1.9 Real Fluid.....	5
1.10 Newtonian Fluid.....	6
1.11 Non-Newtonain Fluid.....	6

1.12 Fluids with Period Dependence.....	6
1.13 Fluids that are Time Independent.....	7
1.14 Prefect Plastic Fluid.....	7.
1.15 Thixotropic Fluid.....	7
1.16 Gas.....	8
1.17 Liquid.....	8
1.18 Compressible Fluid.....	8
1.19 Incompressible Fluid.....	9
1.20 Peristaltic Fluid.....	9
1.21 MHD.....	9
1.22 Thesis Contribution .....	10
1.23 Thesis Organization .....	11
CHAPTER 2.....	12
LITERATURE REVIEW.....	12
CHAPTER 3.....	18
BASIC DEFINITION AND FORMULAS .....	18
3.1 Fluid .....	18
3.2 Newtonian Fluid .....	18
3.3 Non Newtonain Fluid .....	18
3.4 Viscoelastic Fluid .....	18
3.5 Compressible and Incompressible Fluid.....	19
3.6 Time-Dependent Fluid .....	20
3.7 Time-Independent Fluid.....	20
3.8 Peristaltic Flow.....	20
3.9 Walters' B fluid .....	21
3.10 Density.....	21

3.11 Viscosity.....	21
3.12 Newton's Principle of Viscosity.....	21
3.13 Principle of Conservation of Mass.....	22
3.14 Principle of Conservation of Energy.....	22
3.15 Pressure.....	22
3.16 Temperature.....	23
3.17 Stress Tensor.....	23
3.18 Stream Function.....	23
3.19 Chemical Reaction.....	24
3.20 Porosity.....	24
3.21 Heat Transfer.....	24
3.22 Magnetohydrodynamic (MHD).....	25
3.33 Soret and Dufour Parameters.....	26
3.34 Perturbation Method.....	26
CHAPTER 4.....	27
REVIEW WORK.....	27
4.1 Introduction.....	27
4.2 Mathematical Formulation.....	27
4.3 Method of solution.....	34
4.4 Result and discussion.....	37
CHAPTER 5.....	50
CHARACTERISTIC OF PERISTALTIC FLOW OF WALTERS' B FLUID WITH CHEMICAL REACTION AND CONVECTIVE CONDITIONS.....	50
5.1 Introduction.....	50
5.2 Mathematical Formulation.....	50
5.3 Method of solution.....	55

5.4 Result and discussion.....	58
CHAPTER 6.....	66
CONCLUSION AND FUTURE WORK.....	66
6.1 Conclusion .....	66
6.2 Future work.....	67
REFERENCES.....	68

## LIST OF FIGURES

FIGURE NO.	TITLE	PAGE
3.1	Compressible and Incompressible Fluid	19
4.1	The geometry of the problem	28
4.2	Graph show the longitudinal velocity $u$ for various values of the wall properties parameters.	37
4.3	Graph show the longitudinal velocity $u$ for various values of the Eyring-Powell fluid parameter $K$	38
4.4	Graph show the longitudinal velocity $u$ for various values of the parameter $M$ .	38
4.5	Graph shows the temperature $\theta$ for various values of the Dufour number $Du$ .	39
4.6	Graph show the temperature $\theta$ for various values of the Soret number $Sr$ .	39
4.7	Graph show the temperature $\theta$ for various values of the Biot number $\gamma_1$ .	40
4.8	Graph show the temperature $\theta$ for various values of the Biot number $\gamma_2$	40
4.9	Graph shows the concentration $\phi$ for various values of the Dufour number $Du$ .	41
4.10	Graph shows the concentration $\phi$ for various values of the Chemical reaction parameter $\gamma$ .	42
4.11	Graph shows the concentration $\phi$ for various values of the Schmidt number $Sc$ .	42
4.12	Graphs shows the Effects of $E_1$ on the streamline patterns of the fluid.	44
4.13	Graphs shows the Effects of $E_2$ on the streamline patterns of the fluid.	45

4.14	Graph show the Effects of $E_3$ on the streamline patterns of the fluid.	46
4.15	Graph shows the Effects of $K$ on the streamline patterns of the fluid.	47
4.16	Graph show the Effects of $M$ on the streamline patterns of the fluid.	48
5.1	The geometry of the channel	51
5.2	Graph shows the impact of Walters' B Fluid parameter ( $\kappa$ ) on the velocity of the fluid.	58
5.3	Graph shows the impact of porosity parameter ( $K$ ) on the velocity of the fluid.	59
5.4	Graph shows the impact of Reynolds number ( $Re$ ) on the velocity of the fluid.	59
5.5	Graph shows the impact of wavenumber ( $\delta$ ) on the velocity of the fluid.	60
5.6	Graph shows the temperature Profile for $Bi_1$ .	60
5.7	Graph shows the temperature Profile for $Bi_2$ .	61
5.8	Graph shows the temperature Profile for $Br$ .	61
5.9	Graph shows the temperature Profile for $\delta$ .	62
5.10	Graph shows the temperature Profile for $\kappa$ .	62
5.11	Graph shows the temperature Profile for $K$ .	63
5.12	Graph shows the concentration Profile for $\gamma$ .	63
5.13	Graph shows the concentration Profile for $Sr$ .	64

## LIST OF SYMBOLS

$S$	Extra Stress Tensor
$\rho$	Density
$P$	Pressure
$\tau$	Shear Stress
$\mu$	Dynamic Viscosity
$R$	curvature parameter
$c$	Wave Speed
$\lambda$	Wavelength
$M$	Magnetic Field
$\psi$	Stream Function
$u$	Velocity in x- direction
$v$	Velocity in y-direction
$Re$	Reynold Number
$Pr$	Prandtl quantity
$Sr$	Soret Number
$Du$	Dufour Number
$\eta$	Peristaltic Wall
$\epsilon$	Amplitude
$E$	Eckert Number
$\gamma$	Chemical reaction parameter
$k$	Curvature
$\phi$	Inclination of Magnetic Field
$\delta$	wave number
$d_1$	channel thickness
$C$	concentration
$D$	mass diffusivity
$T$	fluid temperature
$K_T$	thermal diffusion ratio
$C_p$	specific heat
$T_0$	temperature at lower wall
$T_1$	temperature at upper wall

$C_0$	concentration at lower wall
$T_0$	climate at the boundaries
$\sigma$	elastic tension

## ACKNOWLEDGMENT

I begin by expressing my profound gratitude to Almighty Allah, whose guidance has made this study both possible and successful. The completion of this study would not have been achievable without the sincere support extended from various sources, for which I am truly thankful. I am particularly indebted to those who played significant roles in my success, with special mention to my research supervisor, Dr. Hadia Tariq. Her unwavering commitment and thorough guidance throughout my research journey was instrumental in the accomplishment of this endeavor.

I shall also acknowledge the extended assistance from the administrations of Department of Mathematics who supported me all through my research experience and simplified the challenges I faced. For all whom I did not mention but I shall not neglect their significant contribution, thanks for everything.

## DEDICATION

*I dedicate this thesis to my loving family, whose unwavering encouragement and sacrifices have been the driving force behind my academic journey. Your support has been my anchor, and this achievement is as much yours as it is mine.*

*To my mentors and educators, your guidance has been invaluable. Your wisdom and encouragement have shaped my intellectual growth, and I am grateful for the knowledge and insights you have shared with me*

# CHAPTER 1

## INTRODUCTION

A fluid is any kind of gas, liquid other substance that flows or frequently expands under a shear stress. For example, water, helium and blood, etc. The analysis of fluid behavior is based on the fundamental rules of mechanics, thermodynamic laws and Mass, momentum and energy are all conserved. The most established physical science that controls both stationary and moving entities impacted by forces is mechanics. The subcategory of fluid dynamics is defining as the branch of engineering science that investigate the behavior of liquid both at still and in action. It consists of liquids, gases, plasmas, and, to a lesser extent, solid polymers.

They can be split into three categories:

1. Statics
2. Kinematics
3. Dynamics

### 1.1 Statics

The study of incompressible fluids in static conditions is known as hydrostatics, and the study of compressible static gases is known as aerostatics.

### 1.2 Kinematics

It controls the motion of the fluid such as displacement, velocity, acceleration and other aspects.

### 1.3 Dynamics

It discusses how fluid velocities and accelerations relate to the forces or energy that drive them. In contrast to fluids, solids are capable of resisting stress from shear through stable deformation. Any amount of shear force will make fluid move, regardless of how little. They move and deform constantly as long as shear stress is applied. It concludes that a liquid at repose must be in a situation of absence of shear force, sometimes referred to as the hydrostatic stress condition. The investigation of the movement of fluids is called fluid mechanics (fluid dynamics). In many areas of science and engineering, fluid mechanics is essential. For example,

Biomechanics: The movement of cerebral fluids, air in the lungs, and blood via arteries and veins.

Households: Pipe and duct networks for heating and air conditioning systems, petroleum gas pipelines and sewage pipelines.

Movements of air currents and water currents are studied in meteorology and ocean engineering.

Syphons, turbines, air-molding hardware, contamination-control equipment and other mechanical engineering plans.

Civil engineering topics include the movement of river sediments, air and water pollution, and flood control techniques.

Vehicle: IC motor, cooling, fuel flow, outside ideal design, etc.

A fluid can be categorized based on the following characteristics:

1. Flow
2. Viscosity
3. Density
4. Compressibility

Fluids are split into four groups based on how they flow and these are:

### 1.4 Steady or Unsteady Fluid

A stable fluid has a density that is constant throughout its entire flow. When a fluid's flow velocity varies between any two locations, such fluid is said to be unstable.

## **1.5 Compressible and Incompressible Fluid**

According to the Mach Number, these fluids are divided into compressible and incompressible categories. According to Mach Number ranges, a fluid is compressible if its ranges are between 0.3 and 1, but incompressible if they are less than 0.3.

## **1.6 Viscose or Non-Viscous Fluid**

Viscose is a term used to describe fluids with a higher viscosity or thickness. Shampoo and motor oil are a couple of examples. The fluids that have a comparatively low thickness or viscosity are considered non-viscous fluids. These fluids exhibit negligible to zero internal friction resistance. Contrary to non-viscous fluids, viscous fluids lose kinetic energy during flow. Superfluid liquid helium is one example.

## **1.7 Rotation or Irrotation Fluid**

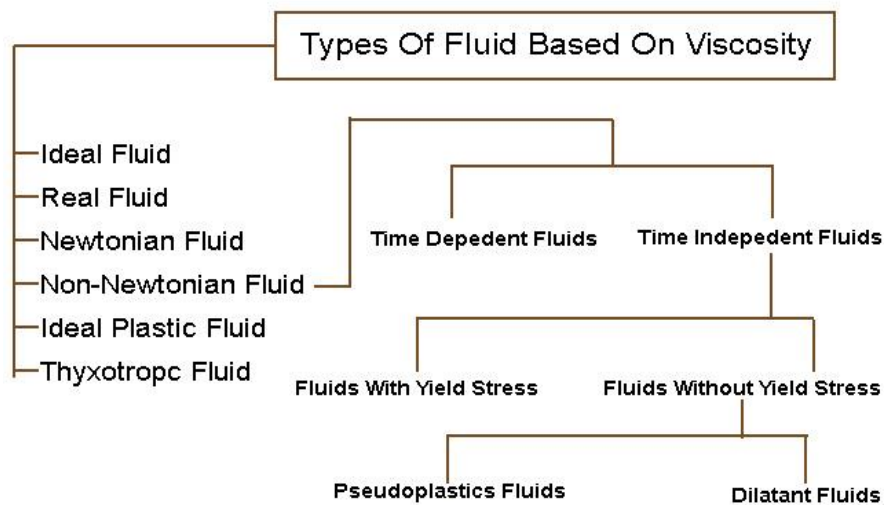
Fluid with rotation or irrotation based on angular motion. There are two categories for the fluid. The first is known as rotating fluid, whereas the second is known as irrotational fluid. The angle is rotational if it fluctuates with the flow. If the fluid spins uniformly and the inclinations between its borders remain constant, the motion of the fluid is said to be irrotational circulation.

Fluids are categorized into the following groups according to their viscosity:

1. Ideal Fluid
2. Real Fluid
3. Newtonian Fluid
4. Non-Newtonian Fluid
5. Perfect Plastic Fluid
6. Thixotropic Fluid

## 1.8 Ideal Fluid

An incompressible liquid is the ideal fluid. There are zero surface tension or viscosity in this kind of fluid. A perfect fluid is another name for the ideal fluid. It is an invented fluid because no fluid in reality possesses these characteristics. Some liquids, such as water, which has a very low viscosity, a low surface tension, and a strong resistance to compression, can be regarded as perfect.



Water can therefore be regarded as a perfect fluid for all practical purposes without introducing a significant amount of inaccuracy.

Any fluid cannot in reality possess these specific characteristics. Every fluid has some surface tension, viscosity and compressibility. Therefore, there isn't a real-world equivalent of a perfect fluid.

## 1.9 Real Fluid

A compressible fluid is the actual fluid. Every real fluid in the universe has some degree of viscosity and surface tension. The term "practical fluid" also refers to a real fluid.

Real fluid, often referred to as practical fluid, is a fluid that possesses characteristics like viscosity, surface tension and compressibility. Every liquid found in nature is actual fluid. Water, petrol, kerosene and other actual fluids are examples.

## **1.10 Newtonian Fluid**

The liquid that abides by Newton's principle of Viscosity is considered to be a Newtonian fluid. When a liquid is a Newtonian, the rate of shear strain and the shear stress are inversely related. The fluid's temperature and pressure have a significant impact on the viscosity as well. Water, hydrogen, emulsions, kerosene and air are a few examples of Newtonian fluids.

## **1.11 Non-Newtonian Fluid**

Non-Newtonian fluids are those that violate Newton's principle of Viscosity. Shear stress and shear strain rate are not inversely related in non-Newtonian fluids. Blood, grease, sugar solutions and many other non-Newtonian fluids are examples.

Additional classifications for non-Newtonian fluid include:

## **1.12 Fluids with Period Dependence**

In this category of non-Newtonian fluid, the shear stress or viscosity varies over time. There are two categories of time-dependent fluids: Rheopectic or Anti-thixotropic and Thixotropic Fluids.

### **1.12.1 Rheopectic or Anti-Thixotropic Fluid**

Because of continuous shear and isothermal circumstances, shear stress or viscosity in rheopectic fluids rises with time.

### **1.12.2 Thixotropic Fluid**

Because of continuous shear and isothermal conditions, shear stress or viscosity in thixotropic fluids reduces over time.

## 1.13 Fluids that are Time Independent

In this category of non-Newtonian fluid, the shear stress or viscosity does not vary over time. There are two categories of time independent fluids exist: Dilatant and Pseudo-plastic fluids.

### 1.13.1 Dilatant Fluids

As greater force is applied, dilatants (shear thickening) become more viscous. Wet sand, starch suspensions, gum solution and aqueous solutions of titanium dioxide are all considered dilatant fluids.

### 1.13.2 Pseudo-plastic Fluids

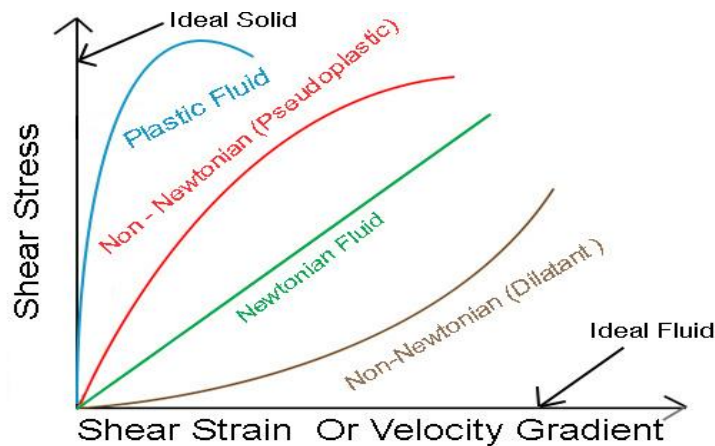
Pseudo-plastics (shear thinning) become less viscous as more force is applied. Nail paint, lava, ketchup and whipped cream are a few examples of pseudo-plastics.

## 1.14 Perfect Plastic Fluid

Based on Newton's Principle of Viscosity, a perfect plastic fluid is one in which the stress under shear is larger than the value of return and the shear force relates to the amount of strain caused by shear. The perfect plastic fluid is often referred to as Bingham Liquid. A yield value of stress under shear is reached by the perfect plastic fluid at which point it starts to flow. Shear stress and velocity gradient have a linear relationship because of how the fluid is moving. Clay water suspension and fly ash are two examples of good polymeric fluids.

## 1.15 Thixotropic Fluid

A fluid is considered to be thixotropic when it starts to flow after reaching a certain yield value of shear stress. When a fluid flows, the connection between the stress caused by shear ( $T$ ) and the speed variation ( $\frac{dy}{dx}$ ) is not constant.



**Shear Stress Vs Shear Strain Graph of Different Types Of Fluids**

The thixotropic fluid resembles plastic fluid up until the point where the shear stress ( $T$ ) starting value surpasses the yield value after that point, however, it does not flow according to Newton's law. Ink and crude oil are two examples of thixotropic fluid.

According to density two categories of fluids are recognized:

## 1.16 Gas

Fluids that don't have a defined shape or volume are called gases. Example: nitrogen and hydrogen.

## 1.17 Liquid

A fluid that has a defined volume but no fixed shape is referred to as a liquid. Example: Oil and water.

The fluid is classified into two categories based on compressibility:

## 1.18 Compressible Fluid

A flexible fluid experiences changes in thickness when a force from outside operates to it.

## **1.19 Incompressible Fluid**

The hardness of a fluid that is incompressible remains unchanged in the presence of an applied force.

## **1.20 Peristaltic Fluid**

Peristaltic transport refers to fluid movement caused by waves created by the symmetric contraction and relaxation of flexible walls. Due to its extensive participation in human physiological processes like sperm movement, blood circulation, urine transport, blood vessel vasomotion, fluid transfer across the perivascular region of the brain and food swallowing in the esophagus, this phenomenon is rather well known. Some significant industrial uses of this technique include lung-heart equipment, kidney equipment and numerous other manmade gadgets. Peristalsis is widely used in a variety of medical and industrial procedures, which encourages researchers to explore it in many circumstances.

## **1.21 MHD**

Magnetohydrodynamics, which studies fluid dynamics using magnetic events, is one of the most intriguing subfields of physics. The phrase "magnetohydrodynamics" is made up of the words "magneto" (which implies a magnetic force), "hydro" (which denotes liquid and "dynamics," which denotes motion). The idea of magnetohydrodynamics was first implemented by Alfven [39]. He is credited with being the one to distinguish astrophysics as a distinct branch of science. Although the non-compressible magnetohydrodynamic fluid was actually born between 1936 and 1937, this was its official birth year. In their theoretical and experimental studies, Hartmann and Lazarus focused on the fluid flow of magnetohydrodynamics through ducts. These magnetic fluids can be, for instance, plasma, liquid metals (like mercury), saltwater and electrolytes. Magnetohydrodynamics plays a significant role in several branches of science, including solar physics where we will study the magnetic hydrodynamics of the sun, astrophysics, etc.

- MHD is used to model the dynamics, equilibrium and macroscopic force balance. Dynamics on large scales is largely described by ideal MHD.
- Plasma stability may be effectively predicted using ideal MHD. One of the intriguing aspects is that the majority of catastrophic instabilities are unstable in optimal MHD. Laboratory plasmas, the solar atmosphere and other phenomena are found to require MHD physics.
- The magnetospheres of the sun, the heliosphere and the earth, along with the gravitational domains of ionized disturbances and neutron galaxy magnetospheres, are systems that MHD rather well describes.
- In most astrophysical plasmas, MHD provides a reassuringly accurate approximation.

Magnetohydrodynamics has downsides of its own, just like every technological advance has advantages and disadvantages. There are some restrictions on the applications of magnetohydrodynamics, therefore it cannot always be helpful.

These are a few of MHD's shortcomings, or more accurately, its constraints.

Magnetohydrodynamics is only partially applicable when

- Effects that are not fluid or kinetic are crucial:
  - Solar wind turbulence dissipating
  - Reconnection of the magnets
  - Dynamics at the nanoscale in the Earth's magnetosphere
- Unlike cosmic rays, the particle distribution functions are not Maxwellian.
- Weak ionization of the plasma:
  - The ionosphere of Earth, the optical sphere and chromosphere of the sun, chemical clouds and a few laboratory plasmas.

## 1.22 Thesis contribution

A thorough review of previous research is provided in this thesis T. Hayat *et al.* [46]. The main points of interest are the properties of Walters' B fluid peristaltic fluids under chemical reaction, magnetohydrodynamics (MHD) and connective boundary conditions effects in an asymmetric porous channel. A suitable transformation technique has been used to reduce the number of dependent variable and perturbation technique to obtain solutions. The study's computational

component made use of Mathematica, and graphical representations will be used to graphically present the results.

### 1.23 Thesis organization

This thesis is further divided into the following chapters, which are as follows:

**Chapter 2** contains a detailed review of the literature.

**Chapter 3** explores the fundamental principles, rules and concepts that are necessary to understand the upcoming work. This chapter concludes with an introduction to the perturbation method and many terms to be used in our research work.

**Chapter 4** provides a review of the work by Hayat *et al.* [46].

**Chapter 5** expands on the research done by Hayat *et al.* [46]. In an asymmetric porous channel, the convective boundary conditions, MHD and chemical reaction are applied on the Walter's B fluid model.

**Chapter 6** contains the conclusion drawn in chapter 5.

Lastly, all of the sources that were used for this research work are included in the reference list.

## CHAPTER 2

### LITERATURE REVIEW

The flow that is brought on by sinusoidally deformed vessel walls is referred to as peristaltic flow. Rhythmic contractions and relaxations of the vessel's smooth muscles are because of peristaltic flows. Many researchers discussed the motion of peristaltic waves. Firstly, the peristaltic movement in a Newtonian fluid was observed by Latham [1]. Various approaches have been used to investigate the behavior of peristaltic in fluid that aren't Newtonian theoretically. Siddiqui *et al.* [2] noticed through tubes how peristaltic flow works in a second-order fluid. In an elliptic cross-section duct, the pattern of peristaltic motion of Casson fluid while taking into account the circulation of mass and heat were observed by Nadeem *et al.* [3]. Also, Nadeem *et al.* [4] examined a third-order fluid in which the interaction of mass and heat in a diverging duct changes the peristaltic circulation. Ellahi *et al.* [5] evaluated the influence of mass and heat exchange on peristaltic motion in an irregular rectangular stream. Mehmood *et al.* [6] explored a modified version of the thermal transfer model to characterize non-Newtonian peristaltic mechanisms thermo-mechanically.

Zeeshan *et al.* [7] focused on the rheological action of difficult peristaltic waves of nanofluid traveling in a rectangular conduit. The analytic answer was discovered once the electrophoresis effect was concentrated. They discovered that the flow is positively impacted by a change in the amplitude ratios of complex waves. Theoretically, Tripathi *et al.* [8] investigated the complicated peristaltic transport-related to nanofluid motion phenomena under the consideration of electro-osmosis. The complicated wave produces the peristaltic movement of viscous fluid along a tube were reported by Javid *et al.* [9]. They assessed the outcomes using numerical simulations. Magnetohydrodynamics was given additional attention in the evaluation, which raised the study's value. Additionally, Tripathi *et al.* [10] noticed how ocular flow is affected by electro-dynamical with little stress fluids. Bhatti *et al.* [11] studied the circulation in a Two-phase via a channel with a suitable wall. Ali *et al.* [12] created a feature

that allows FENE-P fluid to move peristaltically when it travels via an axisymmetric conduit in the core area. They emphasized the impact of electroosmosis. Ali *et al.* [13] showed that the fluid movement of Ellis in the center of the zone was identical.

Tripathi *et al.* [14] created applications for the peristaltic circulation of nanofluids via a thin tube in a spongy atmosphere in blood vessels. Mansour *et al.* [15] looked into how the fluctuation of mass and heat harmed the motion of non-Newtonian fluid during peristalsis in an inconsistent upward pipe. Yih and Fung [16] have mostly studied the peristaltic flow spreading wave propagation of a limited range theoretically. By focusing on the sinusoidal fluctuation at the walls. The behavior of viscous fluid moved peristaltically via a channel and a pipe was studied by Tripathi [17]. Baliga *et al.* [18] analyzed the consequences of slip in velocity and temperature loss on the peristaltic circulation of a Herschel-Bulkley fluid travelling through a homogeneous two-dimensional transparent pipe under the assumptions of an extended wavelength and a low Reynolds quantity. The numerical illustrations for the speed and temperature fields, pressure slope, and stream function have been found via the closed-form solutions of the energy and momentum equations. Numerical integration has been used to calculate the resistive force and pressure growth. The effect of key parameters on the problem has been investigated and graphically displayed. The entrapment phenomena of the Herschel-Bulkley fluid are also investigated. It is observed that the velocity slip parameter increases at the same time as the bolus volume.

Rajashekhar *et al.* [19] investigated the impact of different hemodynamic flow parameters on the mass and heat-driven peristaltic motion of a Ree-Eyring liquid. The equations that underlie the system are nondimensionalized with the aid of correspondence adjustments. The broad variety approximation with an extended wavelength and minimal Reynolds is used to solve the underlying differential equations. Saleem *et al.* [20] observed the physical properties of peristaltic circulation of hybrid nano fluid while passing through the curve duct with ciliated wall. Rafiq *et al.* [21] observed how activation energy and different parameters affected peristaltic flow via a porous wall stream. The focus of this work is on the peristaltic passage of the Jeffrey liquid via a conduit with a porous structure. Magnetohydrodynamic (MHD) effects are taken into account in the problem formulation. Mass transfers are considered in terms of energetic activation and consistent source/sink consequences for heat. A chemical process is also considered in the analysis. The Lubrication approach is used to simplify the analysis of the

succeeding non-linear problems. To discuss the findings graphically for different flow parameters, the MATHEMATICA program NDSolve is utilized. In particular, the blood flow can be studied using the study that is described in the current analysis. Jeffrey's fluid demonstrates the same traits as have been discovered in blood. Abbasi *et al.* [22] looked explored how mass and heat moved over an asymmetric duct during the peristaltic circulation of an Ellis liquid. The modeling process takes into account the characteristics of chemical reactions. The long wavelength is assumed while the small Reynolds number hypothesis is applied to the flow modeling. It is noted how different emergent physical characteristics affect the solutions that are found. Newtonian fluid flows peristaltically across eccentric cylinders as a result of heat transfer analyzed by Puranik *et al.* [23]. Using the perturbation technique, a rough temperature and velocity solution is achieved. A graphical depiction for constant flow rate is used to evaluate how the variation in pressure slope and speed relates to a number of non-dimensional characteristics. A conceptually computed analysis of peristaltic travel in a circular disc with thermal exchange is compared with the existing research at zero inclination to justify the approximation. Endoscopy, which is essential for detecting internal organ problems, has applicability in the current investigation. A catheter's rate of flow must be maintained while being inserted into a blood vessel, and the change in pressure slope helps with this.

Nazeer *et al.* [24] examined the rate of heat exchange of peristaltic travel in an uneven duct utilizing laser and magnetic effects to cure autoimmune disease. In this work, a hybrid Casson liquid nanoflow is covered. Both spherical and platelet-shaped nanoparticles are considered in the conceptual framework. The effects of magnetic fields, viscous dissipation, and Joule heating on electro-osmotic circulation (EOF) in an uneven route are all discussed here. Lubrication factors have also been considered in order to lessen skin friction. In addition, with the aid of heat slip borders and laser rays, a theoretical treatment for rheumatoid arthritis is clearly constructed. A thorough parametric analysis shows that using nanoparticles with a spherical form to treat autoimmune illnesses has shown positive results. Rafiq *et al.* [25] examined how ciliated walls affected the peristaltic circulation of Rabinowitsch liquid in bendable tubes with weight and thermal transmission. In the presence of radiant propagation and connective circumstances at the boundary, the associated mathematical equations are modeled. Also taken into account is mass transfer with Soret effects. The complex group of equations is simplified using the lubrication technique. For shear reduction and stiffening fluid, the impact of various

parameters on velocity is thoroughly discussed individually. There is a drop in temperature near the boundaries because convective heat transmission is found to be stronger there. Alhazmi *et al.* [26] looked at the convection of heat in nanofluids for peristaltic movement in an irregular route. It is described as a magnetic pairing stress nanofluid circulation with dual diffusive convection when peristaltic generate flow occurs in a symmetric irregular duct. The knowledge obtained from the current work will be essential for the development of adaptive magneto-peristaltic engines for specialized thermal and medication transfer processes. Vaidya *et al.* [27] explored an analysis of the flow of blood over an irregular sloping route by considering blood as a non-Newtonian Phan-Thien-Tanner (PTT) solution. The consequences of the chemical interaction and the circumstances surrounding convection are examined in the present approach. In order to imitate the mobility of the particles in operative structures, connections incorporating such constraints report assisting behavior. A perturbation process provides a solution to the complex systems that govern the fluid's path. A variety of physiological traits are thoroughly investigated in relation to different growing factors. A magnetic field is needed for blood flow analysis equipment such as catheters and medication delivery systems. Hemodialysis support is the aim of the pertinent peristaltic model.

Ibrahim *et al.* [28] analyzed the mixed circulation magnet nanoflow of Prandtl fluid via an inconsistent tube with peristalsis. The outside effects of energy generated and non-constant fluctuations in velocity are fully taken into account. Arafa *et al.* [29] looked at how nanofluids moved peristaltically via a porous media. Variable porosity affects the porous medium's permeability and thermal conductivity. The inconsistent nanofluids framework is used to demonstrate how the mixture's characteristics and behaviors of nanofluids rely on the size and shape of the nanoparticles. During the formulation, it is presumable that occurrences of a thermal source/fall as well as the effects of diffuse viscosity will be relevant. The wavy-duct chaos is analyzed, and the irreversibilities of heat transmission and nanofluid friction are compared. Qureshi *et al.* [30] assessed the consequences of a field of magnetic with radial variations on a nanofluid that was peristaltically moving through a limited bendable conduit. The axisymmetric funnel interior is covered in cilia that oscillate in metachronous waves. These metachronal waves, which are produced by cilia in a wavy or beating motion, cause flow. The presence of carbon nanotubes improves the thermal conductivity of water-based fluid. Additionally, heat generating process is combined with heat transport analysis. Adams-Bashforth approach is used to obtain a numerical solution.

Walter [31] proposed Walters' B Model, which is also commonly considered as the non-Newtonian viscoelastic model. Walters' B Model also explains the behavior of extensional polymers and their elastic properties, despite the fact that it produces exceedingly nonlinear equations. Makinde *et al.* [32] discussed the peristaltic movement for Walters' B liquid by taking the consequences of MHD, the slip conditions and heat source under the influence of thermal radiation. Nandeppanavar *et al.* [33] evaluated the heat movement in Walter's B liquid by taking into account an uneven heat source and sink and elastic contraction across an impermeable stretched sheet. By using several heat segmentation techniques, Siddique *et al.* [34] created ferroelectric temperature measurement of Walter's-B liquid. The Walter's-B solution containing peristaltic transport bacteria was investigated by Chu *et al.* [35] in terms of heat flux and micro nanoparticle flow. Tanveer *et al.* [36] analyzed the consequences of heat emission on Walter's B liquid idea in a bent stream with boundary features. Using a pair anxiety framework and an opaque material, Jaafar *et al.* [37] looked into the peristaltic circulation of Walter's B liquid through an unbalanced conduit. The inclination of pressure, action, confined occurrences, speed dispersion, and balance of weight are all modeled using the structural formulation. To get an accurate result, the perturbation approach is used in conjunction with circulation inquiry, which implies a duration with a tiny Reynolds factor. It has been discovered how different factors affect the pressure gradient and velocity distribution of the restricted phenomenon. Jaafar *et al.* [38] examined into and explained how Walter's B solution flows peristaltically in an inclined, unbalanced duct. The balance of weight, momentum, pressure gradient, and temperature distribution can be calculated using models to determine the governing equation. In order to get a precise result, the flow analysis uses the perturbation approach and benefits from the along amplitude and minor Reynolds amount assumptions. The climate gradient and pressure gradient are affected by various factors, as has been found. In the collection of figures, these elements are graphically assessed.

Hannes Alfvén [39] developed the field of MHD. In 1970, he was also awarded by a Noble prize. In fluid dynamics, we describe MHD by Navier-Stokes equations and in electromagnetism, we represent the MHD by Maxwell equations. These differential equations can easily be solved simultaneously. Mallikarjuna *et al.* [40] investigated how MHD flow is affected by thermal slip and velocity in an asymmetric non-uniform duct. The central concept of MHD is that magnetic flux generates electricity to pass through fluids, charges the fluid, and allows electricity to move through them. The fundamental MHD equation is a partial

differential equation. Ali *et al.* [41] noticed how slip affected the peristaltic circulation of a liquid with a range of viscosities in MHD. According to Machireddy *et al.* [42], MHD peristaltic flow is influenced by velocity slip and joule heating via an open medium with chemical interaction. El-dabe and Mostapha [43] studied the effects of MHD on Walter's B liquid simulation passing by a spongy endoscope. The significance of mass and heat exchange on the hydro-magnetic peristaltic circulation of a Casson liquid in a spinning sloped structure via an unbalanced route was examined by Hafez *et al.* [44]. The study conducted by Devakar *et al.* [45] examined the implications of magnetohydrodynamics (MHD) on the peristaltic locomotion of a fluid that is not a Newtonian called a pair-anxiety solution within an apparatus filled with an endoscope. Pair anxiety substance is found in the space between two parallel slanted tubes. It is believed that the interior of the tube is perfectly round and unwavering, whereas the exterior of the tube is a wave with a sinusoidal form. A wave frame traveling at a constant speed is used to discuss fluid motion. This research has numerous bio-medical engineering implications, such as the transport phenomena in peristaltic micro pumps.

## CHAPTER 3

### BASIC DEFINITIONS AND FORMULAS

#### 3.1 Fluid

Fluids are defined as substances that may flow, such as gases (oxygen, hydrogen) and liquids (water, gasoline, honey).

#### 3.2 Newtonian Fluid

No matter how much shear is used; Newtonian fluids maintain a fixed viscosity at a specific temperature. Shear tension and viscosity in these fluids have a linear relationship. Water, alcohol and light motor oil are a few examples.

#### 3.3 Non- Newtonian Fluid

Fluids that are not Newtonian are ones whose density varies and whose response to shear stress is unpredictable. Examples include toothpaste, cheese and butter.

#### 3.4 Viscoelastic Fluid

A viscoelastic fluid is one that combines viscous and elastic components to form a fluid that is not Newtonian. In essence, solvent plus a polymer compose viscoelastic fluids. A few examples

include paints, genetic expulsions, numerous biological solution and other industrial compounds.

### 3.5 Compressible and Incompressible Fluid

Real fluids experience expansion or compression when subjected to external forces, pressure changes, or temperature variations, which results in a change in volume. A fluid whose volume fluctuates has the property of flexibility and is therefore a compressible fluid. Whereas, regardless of contraction or growth, a fluid that is incompressible has an exact volume. It is impossible to find a stiff fluid that is incompressible. However, when flexibility is less of a concern, such as when air or water is moving around us, a flow might be viewed as a fluid that is incompressible flow. The term "ideal fluid" or "perfect fluid" refers to an incompressible fluid without viscosity.

The magnitude of the flexibility effect can be calculated from the flow rate. When wind is moving at a speed of 100 m/s or less, it is thought that the fluid is incompressible and when it is moving at a speed more than 100 m/s, it is thought that the fluid is compressible. Low-velocity wind travels, such as a breeze, are fluids that are incompressible, whereas high-velocity wind travels, such as the flow around a plane, are compressible fluids, as seen in the image below.

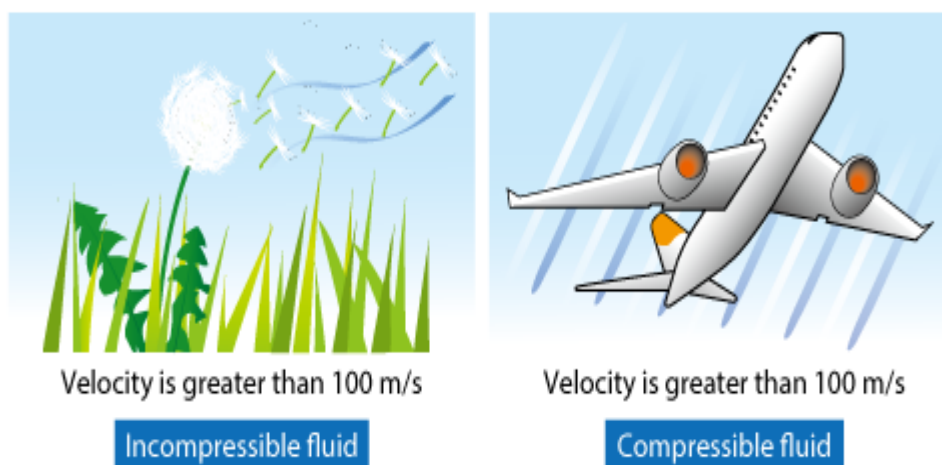


Figure 3.1 Compressible and Incompressible Fluid

### **3.6 Time-Dependent Fluid**

The term "time dependent fluids" refers to fluids whose viscosity depends on the length of flow. The well-known thixotropic fluids fall under this category since they separate into runny and gel phases when disturbed and remain liquid when left alone. Many fluids that are used in both our daily lives and the workplace are time-dependent, including ketchup, mayonnaise, canned baby meals, grease, melts, drilling muds, starches, different kinds of gels, suspensions, polymer solutions and polymer melts.

### **3.7 Time-Independent Fluid**

In fluid dynamics, the term "time-independent fluid flow" describes a situation in which a fluid's flow characteristics do not vary with time. In other words, flow characteristics like temperature, pressure, density and velocity do not change over time. Flow of this kind is frequently referred to as steady-state flow. The consistent flow of water through a conduit is a real-world illustration of time-independent fluid flow. The flow inside the pipe can be regarded as time independent if the water flow rate, pipe diameter and other pertinent parameters stay constant over time. Engineers frequently examine such situations to optimize the design of pipelines for diverse uses, such as water supply systems or industrial processes, assuming steady-state circumstances.

### **3.8 Peristaltic Flow**

A flexible tube or channel's walls contracting and relaxing to move fluid is known as peristalsis. The domains of physiology, business, biology and engineering all heavily rely on this type of fluid transmission. There are several instances, including the movement of chyme through the intestines, the existence of worms and eggs in the female ovary tube, the use of wheel and figure motors, dialysis and the passage of urine from the urinary tract to the bladder.

### 3.9 Walters' B Fluid

One of the better models to represent the properties of a viscoelastic fluid is Walters' B fluid model, which has limiting viscosity at low shear rates and a short memory coefficient.

### 3.10 Density

Density is referring to the weight of a solid object per unit volume. The expression for density is

$$\hat{d} = \frac{\hat{M}}{\hat{V}},$$

where the density is represented by the letter  $\hat{d}$ , volume by  $\hat{V}$  and mass by  $\hat{M}$ .

### 3.11 Viscosity

The resistance of a fluid to bending at a specific rate is measured by its viscosity. It is a common phrase describing the "thickness" of liquids; for instance, syrup is more stiff than water. According to science, viscosity is defined as a force multiplied by a time component divided by an area. As a result, its SI units are newton-seconds per square meter or pascal-seconds.

### 3.12 Newton's Principle of Viscosity

The relationship between a fluid's rate of shear and its stress generated under a mechanical strain is explained in Newton's principle of viscosity. The amount of stress from shear to the shear rate, commonly referred to as the viscosity or factor of thickness, is a constant for a given temperature and pressure. Newtonian fluids adhere to the viscosity law. It is unaffected by the rate of shear. Fluids that are non-Newtonian do not follow Newton's principle, hence their

density (the ratio of the stress of shear to shear rate) is not constant and depends on the rate of shear. The term "dynamic stiffness" refers to the coefficient of thickness, which is determined by Newton's principle of viscosity. The viscosity that is kinematic is calculated by dividing the dynamic stiffness by the volume.

### **3.13 Principle of Conservation of Mass**

The principle of Conservation of Mass is an essential concept of both physics and chemistry, and it claims that no matter what internal processes are going on in a closed system, the system's overall mass remains consistent over time. To put it another way, mass can only transition from one kind to another it is unable to be produced or destroyed. This idea has important applications in physics, chemistry and engineering, among other branches of science.

### **3.14 Principle of Conservation of Energy**

The principle of Conservation of Energy is one of the fundamental concepts of physics. It asserts that the overall energy in a single system remains consistent over time. In simpler terms, energy is unable to be generated or eliminated it is only capable of being transformed into another kind or passed from one object to another. This principle has been tested and validated in a variety of circumstances and is the result of considerable experimental observations. The numerous types of energy include thermal energy, electrical energy, physical energy and various additional types particular to different branches of physics.

### **3.15 Pressure**

A force that is delivered over a certain area is called pressure, and it is frequently expressed in measures like pounds per square inch (*psi*) or pascals (*Pa*). The amount of force per unit area applied orthogonal to an object's surface is referred to as pressure in physics. The following mathematical method can be used to determine pressure (*P*).

$$P = \frac{F}{A},$$

where  $A$  is the region over which the force is exerted,  $F$  is the force that is exerted, and  $P$  is the amount of pressure.

### 3.16 Temperature

The temperature of an object can be used to determine the average energy of motion of its particles. It is a basic physical characteristic that measures how hot or cold a substance is in relation to a common reference point. Various temperature scales are frequently used to measure temperature; the most popular ones are Celsius ( $^{\circ}C$ ), Fahrenheit ( $^{\circ}F$ ), and Kelvin ( $K$ ).

### 3.17 Stress Tensor

A stress tensor is used to examine the distribution of forces within a solid object and how it reacts to loads or deformations from outside the object. It is a key idea in the study of mechanics, particularly in the discipline of continuum mechanics. The distribution of internal forces within a solid object is mathematically represented by a stress tensor in physics and engineering. A material body subject to external forces or deformations has a second-order tensor field that describes the internal stresses and their orientations at every location.

### 3.18 Stream Function

A stream function in fluid dynamics is a mathematical function that is used to explain the motion of a fluid flow in two dimensions. It helps researchers understand irrotational, incompressible flow, in which the fluid's density is constant and its rotating component is absent. The stream equation's partial derivatives give the elements of the fluid circulation's speed and direction, denoted by  $\tilde{\psi}$ , with respect to the coordinates ( $\tilde{x}$  and  $\tilde{y}$ ) as follows

$$u = \frac{\partial \tilde{\psi}}{\partial y} \text{ and } v = -\frac{\partial \tilde{\psi}}{\partial x},$$

where stream function is represented by  $\tilde{\psi}$ ,  $u$  is the component of velocity in horizontal direction and  $v$  is the component of velocity in vertical direction.

### 3.19 Chemical Reaction

An act that transforms a single category of chemical substances into another is known as a chemical reaction. Chemical bonds must be broken and reformed to generate new compounds. The atoms in the reactants undergo reorganization during a chemical reaction to produce products with differing characteristics from the initial materials.

### 3.20 Porosity

The term "porosity" is used in several scientific and technical disciplines to indicate how much void or empty space is present in a material. It denotes the proportion of a material's overall volume to its volume of vacant spaces (pores) and is frequently stated as a percentage. In other words, it measures the percentage of a substance that is made up of empty spaces. In disciplines including geology, soil science, materials science and engineering, porosity is a crucial characteristic since it has a substantial impact on the characteristics and behavior of materials.

### 3.21 Heat Transfer

The transfer of heat is a procedure through which the heat is exchanged across physical structures. Radiation, conduction or convection are all forms of transferring heat.

### **3.21.1 Radiation**

Radiation in the form of waves that are electromagnetic transfers heat energy. Compared to conduction and convection, radiation does not require a medium to transmit heat. All objects with a temperature higher than absolute zero emit heat rays. The temperature of the object and the characteristics of its surface affect how much radiation is emitted. We experience the warmth of a fire even when we are not directly in contact with it because to this form of heat transmission, which is also how the Sun's energy reaches the Earth.

### **3.21.2 Conduction**

Without any movement of the substance itself, conduction is the transmission of heat energy from one molecule to another within a substance. To put it another way, it happens whenever two objects with different temperatures come into touch. Until thermal equilibrium is attained, the heat energy transfers from the hotter to the cooler object. In general, metals are efficient heat conductors.

### **3.21.3 Convective**

Convection is the movement of liquids or gases that transfers heat energy. It takes place in fluids (liquids and gases) when warmer, lighter stuff climbs and colder, denser object falls. As a result, the fluid circulates continuously, transferring heat from one location to another. Ocean currents and weather patterns are caused by convection currents in the Earth's atmosphere and oceans.

### **3.22 Magnetohydrodynamics (MHD)**

Magnetohydrodynamics is an inquiry of the properties and behavior of electrically moving materials with respect to magnetic fields. MHD is sometimes known as hydromagnetics or magneto-fluid dynamics. Examples of these magnetic fluids include electrolytes, salt water, plasmas and liquid metals.

### **3.23 Soret and Dufour Parameters**

The Soret and Dufour parameters are thermophysical characteristics that define the response of heat exchange and mass in fluid systems, notably in the context of transport phenomena and convection-diffusion processes. These variables are crucial in numerous engineering and scientific applications and are frequently employed in assessments of fluid dynamics, heat transfer and mass transfer.

### **3.24 Perturbation Method**

Perturbation methods are mathematical approaches for approximating answers to difficult mathematical problems, especially when those equations include a small or big parameter. These techniques are widely used in many scientific and technical disciplines, including physics, fluid dynamics, quantum mechanics and celestial mechanics, where precise answers are frequently challenging to find.

The fundamental goal of perturbation methods is to eliminate the difficulty of a problem by assuming that the structure may be split into two parts: a known part and a minor perturbation that alters the known part. The perturbation's size is represented by the tiny parameter, commonly written as  $\epsilon$ .

## CHAPTER 4

# EFFECTS OF CONVECTIVE CONDITIONS AND CHEMICAL REACTION ON PERISTALTIC FLOW OF EYRING-POWELL FLUID

### 4.1 INTRODUCTION

In this chapter, we have reviewed the article by Hayat *et al.* [46] entitled “Effects of convective conditions and chemical reaction on peristaltic flow of Eyring-Powell fluid”. This paper discusses the peristaltic flow of Eyring-Powell liquid in a symmetric channel under convective conditions. The consequences of Soret and Dufour are discussed. Assuming the concepts of a small Reynolds quantity and an extended wavelength, the resulting problem has been explored for the temperature, concentration and velocity of the fluid. The results are illustrated graphically and explained in detail for several pertinent parameters.

### 4.2 MATHEMATICAL FORMULATION

This article examines the flow of incompressible Eyring Powell fluid in a two-dimensional, horizontal channel with width  $2d$ . Assuming that waves flow parallel to the  $x$ -direction, we take Cartesian coordinates into account. The  $x$ - and  $y$ -axes are taken transversely in this instance. Channel walls are pliable due to the effects of viscous damping. The waves are considered to have a wavelength of  $\lambda$ .

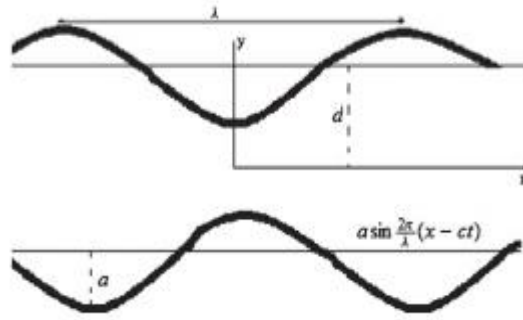


Figure 4.1 The geometry of the problem.

The wall's geometry is described by the expression given below:

$$y = \pm\eta(x, t) = d + a \sin \frac{2\pi}{\lambda} (x - ct), \quad (4.1)$$

where the wave parameters are  $c$  for wave speed,  $a$  for wave amplitude,  $\lambda$  for wavelength,  $2d$  for symmetric channel width,  $t$  for time, and  $\eta$  for upper wall displacement and  $-\eta$  for lower wall displacement. The fluid that is incompressible the continuity equation is given by

$$\text{div } \mathbf{V} = 0. \quad (4.2)$$

The equation for momentum is

$$\rho \frac{d\mathbf{V}}{dt} = -\nabla p + \text{div } \mathbf{S}, \quad (4.3)$$

where material time derivative ( $\frac{d}{dt}$ ), the velocity components  $\mathbf{V} = (u, v)$ , where  $u$  is in  $x$ -direction and  $v$  is in  $y$ -direction, density of liquid ( $\rho$ ) and extra stress tensor ( $\mathbf{S}$ ).

The following is the energy and mass equation incorporating the Soret and Dufour effects:

$$\rho c_p \frac{dT}{dt} = k \nabla^2 T + \frac{Dk_T}{c_s} (\nabla^2 C), \quad (4.4)$$

$$\frac{dC}{dt} = D\nabla^2 C + \frac{Dk_T}{T_m}(\nabla^2 T) - k_1(C - C_0), \quad (4.5)$$

where material time derivative ( $\frac{d}{dt}$ ), density of liquid ( $\rho$ ), chemical response component ( $k_1$ ), concentration susceptibility ( $c_s$ ), amount of heat diffusion ( $K_T$ ), liquid humidity ( $T$ ), weight quantity ( $C$ ), climate at the boundaries ( $T_0$ ), lower border quantity ( $C_0$ ) and upper border quantity ( $C_1$ ), mean humidity of liquid ( $T_m$ ), the factor of weight diffusivity ( $D$ ), particular thermal at fixed pressure ( $c_p$ ) heat conductivity ( $k$ ) and  $\nabla^2 = (\frac{\partial^2}{\partial x^2} + \frac{\partial^2}{\partial y^2})$ .

The Eyring-Powell fluid additional stress tensor is provided as follow:

$$S_{ij} = \mu \frac{\partial u_i}{\partial x_j} + \frac{1}{\beta} \sinh^{-1}\left(\frac{1}{c_1} \frac{\partial u_i}{\partial x_j}\right), \quad (i, j = 1, 2), \quad (4.6)$$

where  $u_1 = u, u_2 = v, x_1 = x$  and  $x_2 = y$ . Also

$$\sinh^{-1}\left(\frac{1}{c_1} \frac{\partial u_i}{\partial x_j}\right) = \frac{1}{c_1} \frac{\partial u_i}{\partial x_j} - \frac{1}{6} \left(\frac{1}{c_1} \frac{\partial u_i}{\partial x_j}\right)^3, \quad (4.7)$$

$$\left| \frac{1}{c_1} \frac{\partial u_i}{\partial x_j} \right| \ll 1. \quad (4.8)$$

Equation (4.6) in component form yields

$$S_{xx} = \mu \frac{\partial u}{\partial x} + \frac{1}{\beta} \left[ \frac{1}{c_1} \frac{\partial u}{\partial x} - \frac{1}{6c_1^3} \left(\frac{\partial u}{\partial x}\right)^3 \right], \quad (4.9)$$

$$S_{xy} = \mu \frac{\partial u}{\partial y} + \frac{1}{\beta} \left[ \frac{1}{c_1} \frac{\partial u}{\partial y} - \frac{1}{6c_1^3} \left(\frac{\partial u}{\partial y}\right)^3 \right], \quad (4.10)$$

$$S_{yx} = \mu \frac{\partial v}{\partial x} + \frac{1}{\beta} \left[ \frac{1}{c_1} \frac{\partial v}{\partial x} - \frac{1}{6c_1^3} \left( \frac{\partial v}{\partial x} \right)^3 \right], \quad (4.11)$$

$$S_{yy} = \mu \frac{\partial v}{\partial y} + \frac{1}{\beta} \left[ \frac{1}{c_1} \frac{\partial v}{\partial y} - \frac{1}{6c_1^3} \left( \frac{\partial v}{\partial y} \right)^3 \right], \quad (4.12)$$

where  $\beta$  and  $c_1$  is material liquid factors of Eyring-Powell.

The transfer of heat is accomplished at the walls by

$$k \frac{\partial T}{\partial y} = -h_1(T - T_0), \quad \text{at } y = \eta, \quad (4.13)$$

$$k \frac{\partial T}{\partial y} = -h_2(T_0 - T), \quad \text{at } y = -\eta. \quad (4.14)$$

The heat transfer coefficients at the upper and lower walls are shown here by the variables  $h_1$  and  $h_2$ , respectively. The following formulations illustrate the no-slip requirement at the walls:

$$u = 0, v = \pm \eta_1, \quad \text{at } y = \pm \eta. \quad (4.15)$$

Additionally, the concentration parameters are provided by

$$C = \begin{Bmatrix} C_1 \\ C_0 \end{Bmatrix}, \quad \text{at } y = \pm \eta. \quad (4.16)$$

Because of this consistency of stress, the force that the boundaries apply to the liquid is equal to and directed in the reverse path from the force that the liquid applies to the boundaries. Furthermore, identical transverse wall displacements at instantaneous locations correspond to equivalent  $y$  fluid displacements. Accordingly, boundary separation is not produced as long as the stress and deformation conditions persist. One can therefore write mathematically.

$$\left[ -\tau \frac{\partial^3}{\partial x^3} + m_1 \frac{\partial^3}{\partial x \partial t^2} + d' \frac{\partial^2}{\partial t \partial x} \right] \eta = -\rho \frac{du}{dt} + \frac{\partial S_{xx}}{\partial x} + \frac{\partial S_{xy}}{\partial y}, \quad \text{at } y = \pm \eta.$$

where  $\tau$  is the elastic tension in the membrane,  $m_1$  the mass per unit area and  $d'$  the coefficient of viscous damping.

Through Equation (4.3), the governing equations are:

$$\rho \frac{du}{dt} = -\frac{\partial p}{\partial x} + \frac{\partial S_{xx}}{\partial x} + \frac{\partial S_{xy}}{\partial y}, \quad (4.17)$$

$$\rho \frac{dv}{dt} = -\frac{\partial p}{\partial y} + \frac{\partial S_{yx}}{\partial x} + \frac{\partial S_{yy}}{\partial y}. \quad (4.18)$$

Creating the subsequent dimensionless variables and introducing the stream functions  $\psi(x, y, t)$ :

$$\begin{aligned} u &= \frac{\partial \psi}{\partial y}, v = -\frac{\partial \psi}{\partial x}, \psi^* = \frac{\psi}{cd}, x^* = \frac{x}{\lambda}, y^* = \frac{y}{d}, t^* = \frac{ct}{\lambda}, \eta^* = \\ &\frac{\eta}{d}, k_1 = \frac{d^2}{v}, \theta = \frac{T-T_0}{T_0}, \Phi = \frac{c-c_0}{c_1-c_0}, S_{xx}^* = \frac{d}{\mu c} S_{xx}, S_{xy}^* = \frac{d}{\mu c} S_{xy}, \\ S_{yx}^* &= \frac{d}{\mu c} S_{yx}, S_{yy}^* = \frac{d}{\mu c} S_{yy}. \end{aligned} \quad (4.19)$$

After dropping (\*) we arrive at:

$$S_{xx} = \delta \psi_{yx} (1 + M) - \delta^3 K \psi_{yx}^3, \quad (4.20)$$

$$S_{xy} = \psi_{yy} (1 + M) - K \psi_{yy}^3, \quad (4.21)$$

$$S_{yx} = -\delta^2 \psi_{xx} (1 + M) + \delta^6 K \psi_{xx}^3, \quad (4.22)$$

$$S_{yy} = -\delta \psi_{yx} (1 + M) + \delta^3 K \psi_{yx}^3. \quad (4.23)$$

Equations (4.2), (4.3), (4.4), (4.5), (4.17), (4.18) and (4.19) yield:

$$\delta Re \left[ \frac{d}{dt} \left( \frac{\partial^2 \psi}{\partial y^2} + \delta^2 \frac{\partial^2 \psi}{\partial x^2} \right) \right] = \delta \frac{\partial^2 S_{xx}}{\partial y \partial x} + \delta^2 \frac{\partial^2 S_{yx}}{\partial x^2} + \frac{\partial^2 S_{xy}}{\partial y^2} - \delta^2 \frac{\partial^2 S_{yy}}{\partial x \partial y}, \quad (4.24)$$

$$\delta Pr Re \frac{d}{dt} \theta = \delta^2 \frac{\partial^2 \theta}{\partial x^2} + \frac{\partial^2 \theta}{\partial y^2} + Pr Du \left[ \delta^2 \frac{\partial^2 \theta}{\partial x^2} + \frac{\partial^2 \theta}{\partial y^2} \right], \quad (4.25)$$

$$\frac{1}{Sc} \frac{\partial^2 \theta}{\partial y^2} + Sr \frac{\partial^2 \theta}{\partial y^2} - \gamma \theta = 0, \quad (4.26)$$

with the conditions in the non-dimensional form are:

$$\eta = 1 + \epsilon \sin 2\pi (x - t), \quad (4.27)$$

$$\theta_y + \gamma_1 \theta = 0 \text{ at } y = \eta, \quad (4.28)$$

$$\theta_y - \gamma_2 \theta = 0 \text{ at } y = -\eta, \quad (4.29)$$

$$\theta = \begin{Bmatrix} 1 \\ 0 \end{Bmatrix}, \quad \text{at } y = \pm \eta, \quad (4.30)$$

$$\psi_y = 0, \quad \text{at } y = \pm \eta, \quad (4.31)$$

$$\left[ E_1 \frac{\partial^3}{\partial x^3} + E_2 \frac{\partial^3}{\partial x \partial t^2} + E_3 \frac{\partial^2}{\partial x \partial t} \right] \eta = \delta \frac{\partial}{\partial x} S_{xx} + \frac{\partial}{\partial y} S_{xy}, \quad \text{at } y = \pm \eta. \quad (4.32)$$

$$\begin{aligned} \delta &= \frac{d}{\lambda}, \quad Re = \frac{cd}{\nu}, \quad Pr = \frac{\mu c_p}{k}, \quad \epsilon = \frac{a}{d}, \quad \gamma = \frac{k_1 d^2}{\nu}, \quad E = \frac{c^2}{T_0 c_p}, \quad E_1 = \\ &= -\frac{\tau d^3}{\lambda^3 \mu c}, \quad E_2 = \frac{m_1 c d^3}{\lambda^3 \mu}, \quad E_3 = \frac{d^3 d'}{\mu \lambda^2}, \quad Sc = \frac{\mu}{\rho D}, \quad M = \frac{1}{\mu \beta c_1}, \quad K = \\ &= \frac{Mc^2}{6d^2 \mu c_1^2}, \quad Du = \frac{DK_T(C_1 - C_0)}{c_s c_p \nu T_0}, \quad Sr = \frac{DK_T T_0}{\nu T_m (C_1 - C_0)}, \quad \gamma_1 = \frac{h_1 d}{k}, \quad \gamma_2 = \frac{h_2 d}{k}. \end{aligned} \quad (4.33)$$

The following definitions apply to the dimensionless oscillation amount ( $\delta$ ), Schmidt quantity ( $Sc$ ), Soret quantity ( $Sr$ ), Dufour quantity ( $Du$ ), Biot quantities ( $\gamma_1$  and  $\gamma_2$ ), and liquid factors ( $M$  and  $K$ ), Reynolds quantity ( $Re$ ), Prandtl quantity ( $Pr$ ), Eckert quantity ( $E$ ), amplitude value ( $\epsilon$ ), chemical response factor ( $\gamma$ ), non-dimensional elasticity factors ( $E1, E2, E3$ ).

Taking into account smaller Reynolds numbers and extended wavelengths, the equations result as:

$$(1+M) \frac{\partial^4 \psi}{\partial y^4} - 6K \frac{\partial^2 \psi}{\partial y^2} \left( \frac{\partial^3 \psi}{\partial y^3} \right)^2 - 3K \left( \frac{\partial^2 \psi}{\partial y^2} \right)^2 \frac{\partial^4 \psi}{\partial y^4} = 0, \quad (4.34)$$

$$\frac{\partial^2 \theta}{\partial y^2} + Pr Du \frac{\partial^2 \phi}{\partial y^2} = 0, \quad (4.35)$$

$$Sr \frac{\partial^2 \theta}{\partial y^2} + \frac{1}{Sc} \frac{\partial^2 \phi}{\partial y^2} - \gamma \phi = 0, \quad (4.36)$$

with corresponding boundary conditions:

$$\psi_y = 0, \quad at \quad y = \pm \eta, \quad (4.37)$$

$$\theta_y + \gamma_1 \theta = 0, \quad at \quad y = \eta,$$

$$\theta_y - \gamma_2 \theta = 0, \quad at \quad y = -\eta, \quad (4.38)$$

$$\phi = \begin{Bmatrix} 1 \\ 0 \end{Bmatrix}, \quad at \quad y = \pm \eta, \quad (4.39)$$

$$\left[ E_1 \frac{\partial^3}{\partial x^3} + E_2 \frac{\partial^3}{\partial x \partial t^2} + E_3 \frac{\partial^2}{\partial x \partial t} \right] \eta = (1+M) \frac{\partial^3 \psi}{\partial y^3} - 3K \left( \frac{\partial^2 \psi}{\partial y^2} \right)^2 \frac{\partial^3 \psi}{\partial y^3}, \quad at \quad y = \pm \eta. \quad (4.40)$$

### 4.3 METHOD OF SOLUTION

Equations (4.35–4.36) that result with conditions (4.38–4.39) have the following precise solutions:

$$\theta = \frac{1}{2} \times Du Pr (L_4 + L_2 y \operatorname{csch}(L_2 \eta) + \operatorname{sech}(L_2 \eta) - \operatorname{cosh}(L_2 \eta) \operatorname{sech}(L_2 \eta) - \operatorname{csch}(L_2 \eta) \sinh(L_2 \eta) - L_5 y),$$

$$\emptyset = \operatorname{csch}(2L_2 \eta) \sinh(L_2 (y + \eta)).$$

The wall's heat transfer coefficient is provided by

$$Z = \eta_x \theta_y(\eta),$$

$$= \frac{\eta_x Du Pr [-L_2 \operatorname{coth}(L_2 \eta) + L_2 \operatorname{csch}(L_2 \eta) - L_5 - L_2 \tanh(L_2 \eta)]}{2}. \quad (4.41)$$

Because of the resultant equation's nonlinear structure (4.34). The closed form solution to this equation for arbitrary values of the parameters seems to be quite difficult to obtain. Thus we focus on the perturbation solution for the small fluid parameter  $K$ . In series form, we do this by expanding the stream function  $\psi$  as follows:

$$\psi = \psi_0 + K\psi_1 + O(K^2).$$

#### 4.3.1 ZEROETH ORDER SYSTEM AND SOLUTION

At the zeroth order, the resultant equation is provided by:

$$\frac{\partial^4 \psi_0}{\partial y^4} = 0, \quad (4.42)$$

$$\psi_{0y} = 0, \quad \text{at } y = \pm \eta, \quad (4.43)$$

$$\left[ E_1 \frac{\partial^3}{\partial x^3} + E_2 \frac{\partial^3}{\partial x \partial t^2} + E_3 \frac{\partial^2}{\partial x \partial t} \right] \eta = (1 + M) \psi_{0yyy}. \quad \text{at } y = \pm \eta. \quad (4.44)$$

When the boundary conditions (4.43–4.44) are used, the solution to equation (4.42) is

$$\psi_0 = y \left( \frac{Ly^2}{3} - L^2 \right). \quad (4.45)$$

Note that solution equations for the zeroth order system match viscous fluid results when Soret and Dufour effects are not present for the given surface temperature.

### 4.3.2 FIRST ORDER SYSTEM AND SOLUTION

The first order system of equation with the boundary condition is given as follow:

$$(1+M) \frac{\partial^4 \psi_1}{\partial y^4} - 6 \frac{\partial^2 \psi_0}{\partial y^2} \left( \frac{\partial^3 \psi_0}{\partial y^3} \right)^2 - 3 \left( \frac{\partial^2 \psi_0}{\partial y^2} \right)^2 \frac{\partial^4 \psi_0}{\partial y^4} = 0, \quad (4.46)$$

$$\psi_{1y} = 0, \quad \text{at } y = \pm \eta, \quad (4.47)$$

$$(1+M) \frac{\partial^3 \psi_1}{\partial y^3} - 3 \left( \frac{\partial^2 \psi_0}{\partial y^2} \right)^2 \frac{\partial^3 \psi_0}{\partial y^3} = 0, \quad \text{at } y = \pm \eta. \quad (4.48)$$

The answer for  $\psi_1$  is obtained as follow by solving the resulting equations (4.46) and then applying the appropriate boundary conditions:

$$\psi_1 = Ay \left( \eta^4 - \frac{y^4}{5} \right), \quad (4.49)$$

where,

$$L = \frac{2\pi^2 \epsilon (-2(E_1 + E_2)\pi \cos 2\pi(x-t) + E_3 \sin 2\pi(x-t))}{(1+M)},$$

$$L_1 = L(1 + \epsilon \sin 2\pi(x-t))^2,$$

$$L_2 = \frac{\sqrt{Sc\gamma}}{\sqrt{1 - Du Pr Sc Sr}},$$

$$L_3 = (-1 + Du Pr Sc Sr),$$

$$L_4 = \frac{2}{L_3(\gamma_1 + \gamma_2 + 2\gamma_1\gamma_2\eta)} \times \left( -\sqrt{Sc\gamma L_3} (1 + \gamma_2\eta) \coth(2L_2\eta) + \sqrt{-Sc\gamma L_3} (1 + \gamma_1\eta) \operatorname{csch}(2L_2\eta) + \frac{1}{2} L_3 \{2\gamma_1 + 2\gamma_1\gamma_2\eta - (\gamma_1 + \gamma_2 + 2\gamma_1\gamma_2\eta) \operatorname{sech}(L_2\eta)\} \right),$$

$$L_5 = \frac{2\sqrt{\gamma - Du Pr Sc Sr\gamma} \operatorname{csch}(2L_2\eta)}{L_3\gamma(\gamma_1 + \gamma_2 + 2\gamma_1\gamma_2\eta)} \times \left( \sqrt{Sc\gamma\gamma_1} - \sqrt{Sc\gamma} (\gamma_1 + \gamma_2 + 2\gamma_1\gamma_2\eta) \cosh(L_2\eta) + \sqrt{Sc\gamma\gamma_2} \cosh(2L_2\eta) + \sqrt{\gamma - Du Pr Sc Sr\gamma_1\gamma_2} \sinh(2L_2\eta) \right),$$

$$A = \frac{16\pi^6 \epsilon^3 (2(E_1 + E_2)\pi \cos 2\pi(x-t) - E_3 \sin 2\pi(x-t))^3}{(1+M)^4}.$$

#### 4.4 RESULTS AND DISCUSSION

This section aims to evaluate the response of the factors that make up the temperature ( $\theta$ ),

longitudinal velocity ( $u$ ), mass concentration ( $\phi$ ), coefficient of heat transfer ( $Z$ ) and stream function ( $\psi$ ). Particularly, the fluctuations in the membrane's elastic tension ( $E_1$ ), the mass per unit area ( $E_2$ ), the viscosity coefficient, and damping ( $E_3$ ), the Schmidt quantity ( $Sc$ ), and the Prandtl quantity ( $Pr$ ), the Dufour quantity ( $Du$ ) and the Soret value ( $Sr$ ), the Biot values ( $\gamma_1$  at the bottom wall and  $\gamma_2$  at the upper wall), as well as the  $\gamma$  chemical reaction parameter are taken into account. The outcomes are presented and assessed via plots.

#### 4.4.1 Velocity and temperature profiles

The purpose of this part is to demonstrate how different developing characteristics affect the velocity  $u$  and temperature profile  $\theta$ . The consequences of wall membrane characteristics ( $E_1$ ,  $E_2$ , and  $E_3$ ) on velocity  $u$  are shown in Figure 4.2. The velocity profile grows as  $E_1$  and  $E_2$  increase. Walls provide an easier path to flow because due enhancement of mass characterizing parameter and elastic tension, which increases speed. The wall's damping properties are demonstrated by the coefficient of viscous damping,  $E_3$ . It offers enough flow friction to reduce speed.

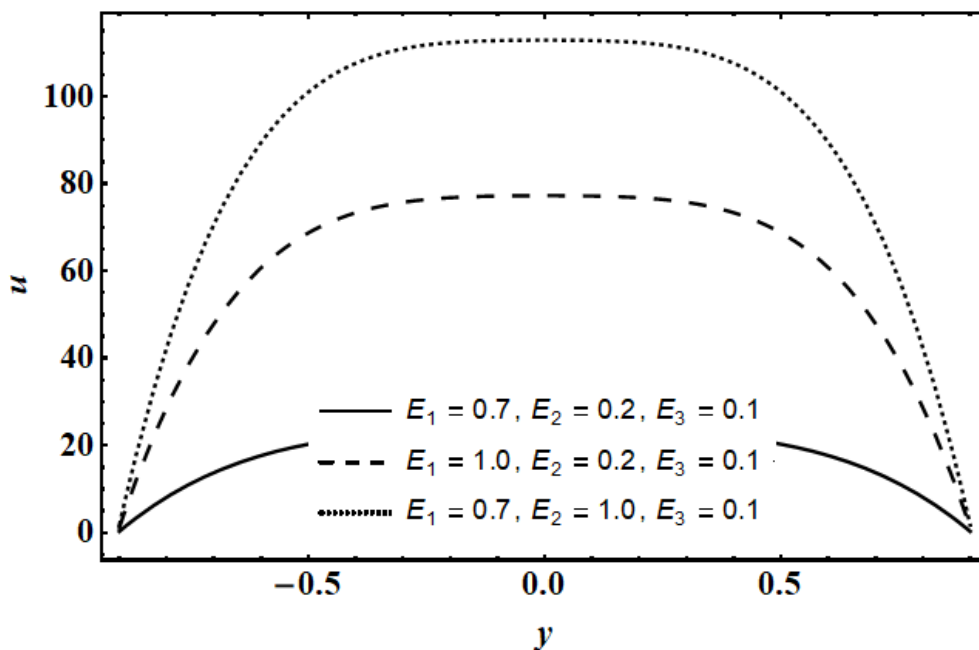


Fig 4.2 Plot of longitudinal velocity  $u$  for various values of the wall properties parameters.

Figures (4.3 and 4.4) demonstrate how the velocity profile drops with small  $K$  and increases with a decline in  $M$ , which is indicative of an Eyring-Powell liquid.

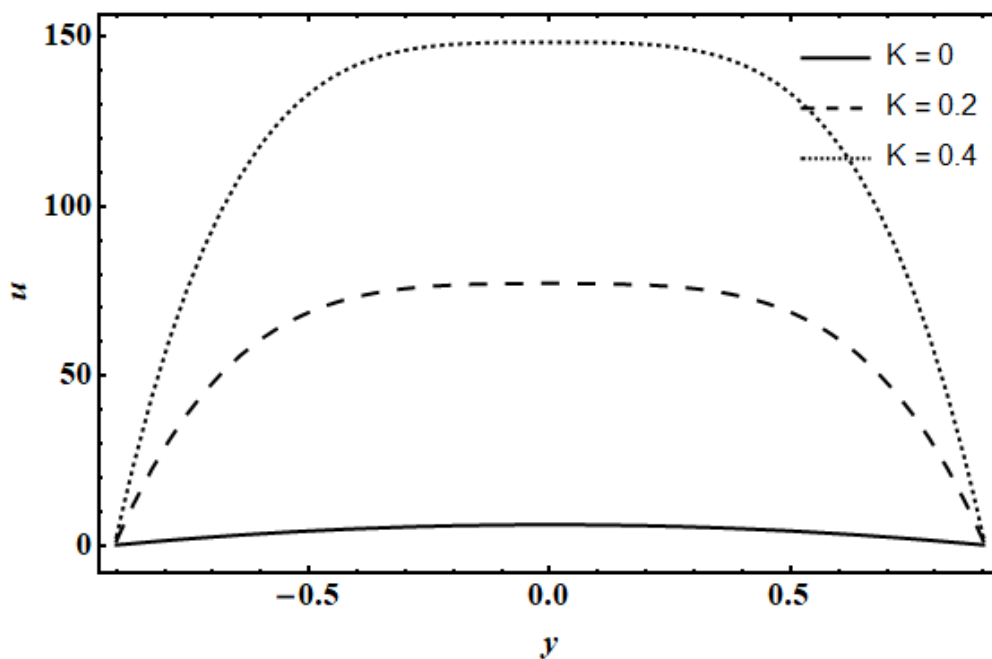


Fig 4.3 Plot of longitudinal velocity  $u$  for various values of the Eyring-Powell fluid parameter  $K$ .

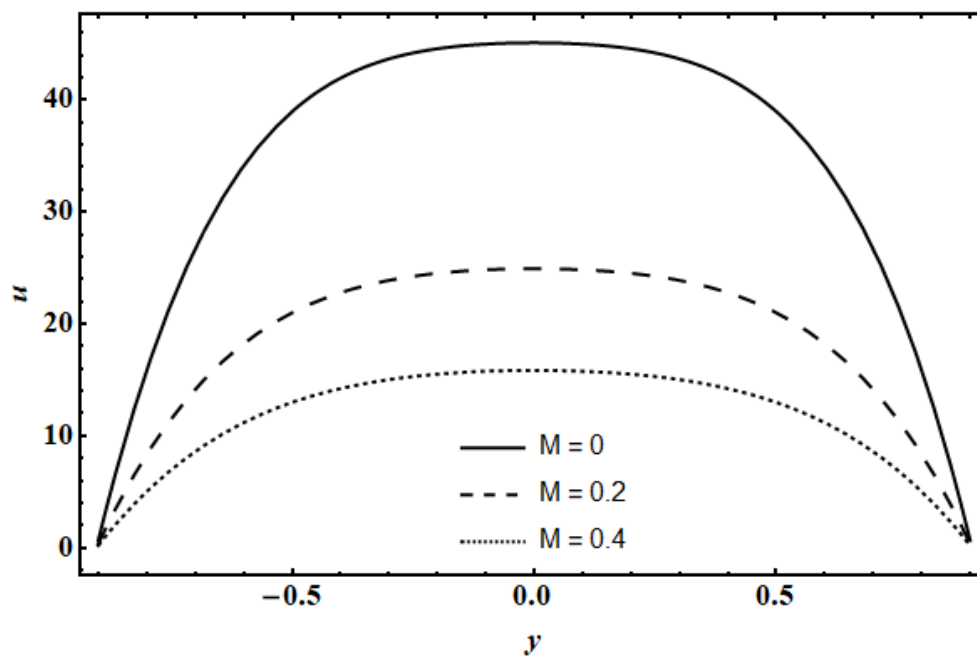


Fig 4.4 Plot of longitudinal velocity  $u$  for various values of the parameter  $M$ .

The consequences of Soret quantity  $Sr$  and Dufour quantity  $Du$  on the temperature profile are examined in Figures 4.5 and 4.6. The temperature drops as the values of  $Du$  and  $Sr$  rise, according to the graphic results. The repercussions of Soret quantity  $Sr$ , however, are more noticeable. It is evident that a rise in  $Du$  lowers the wall's temperature, which lowers the thermal barrier layer. A rise in  $Sr$  lowers the fluid's mean free temperature, which lowers the thermal limit.

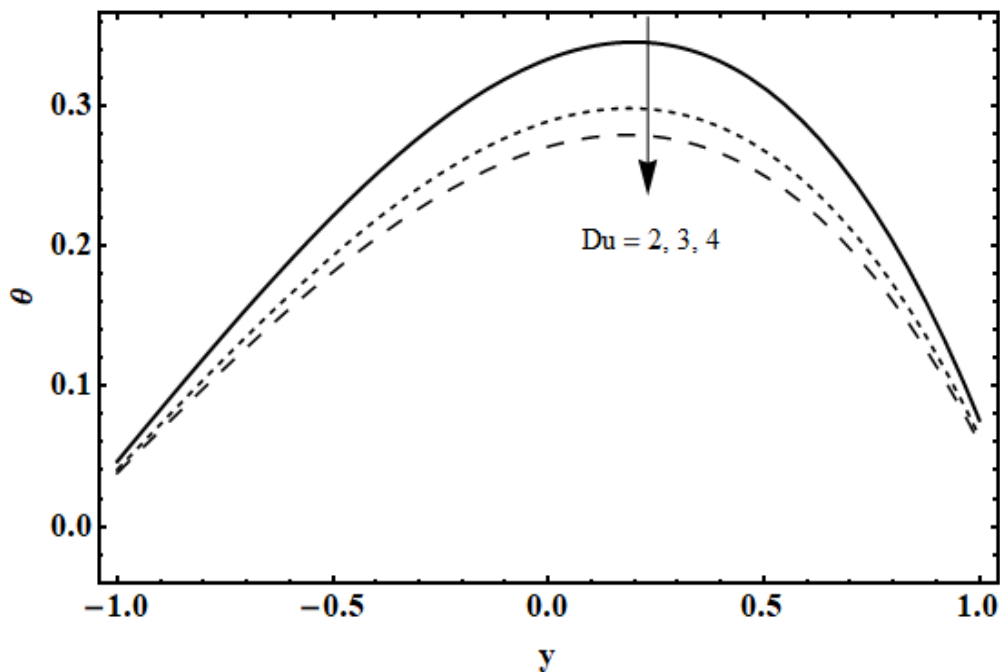


Fig 4.5 Plot of the temperature  $\theta$  for various values of the Dufour number  $Du$ .

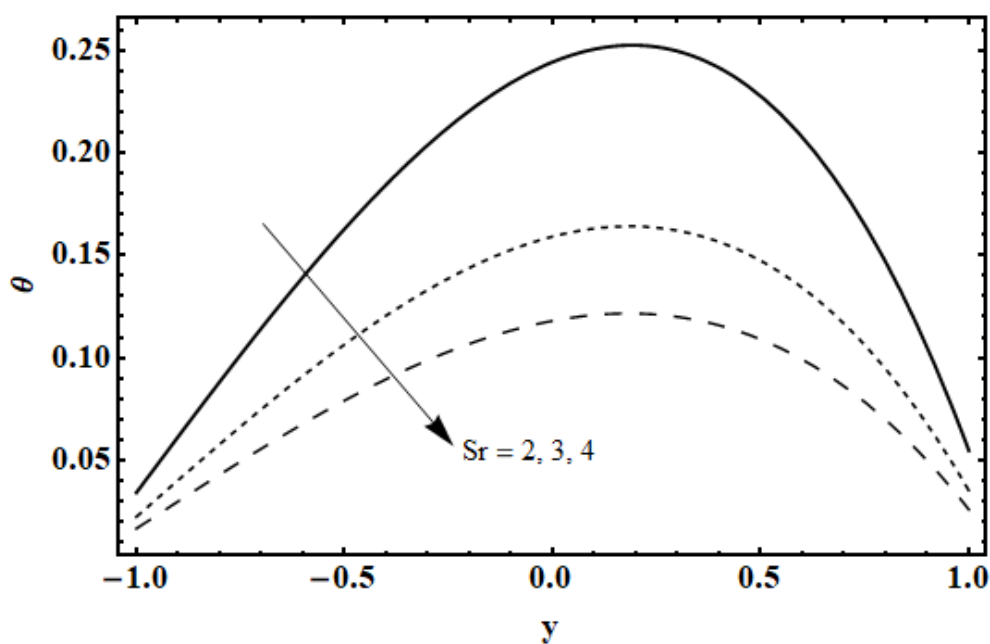


Fig 4.6 Plot of the temperature  $\theta$  for various values of the Soret number  $Sr$ .

Figures 4.7 and 4.8 illustrate the consequences of Biot factors  $\gamma_1$  and  $\gamma_2$ . Because the temperature domain of the liquid is not uniform, the Biot values are chosen to be bigger than one. Conversely, because of the fluid's consistent temperature fields, problems with low Biot values are thermally easy. The obtained results show that when the number of Biot on the lower and top walls increases, the temperature profile decreases. The temperature decline at the border is justified because thermal conductivity reduces as Biot number increases.

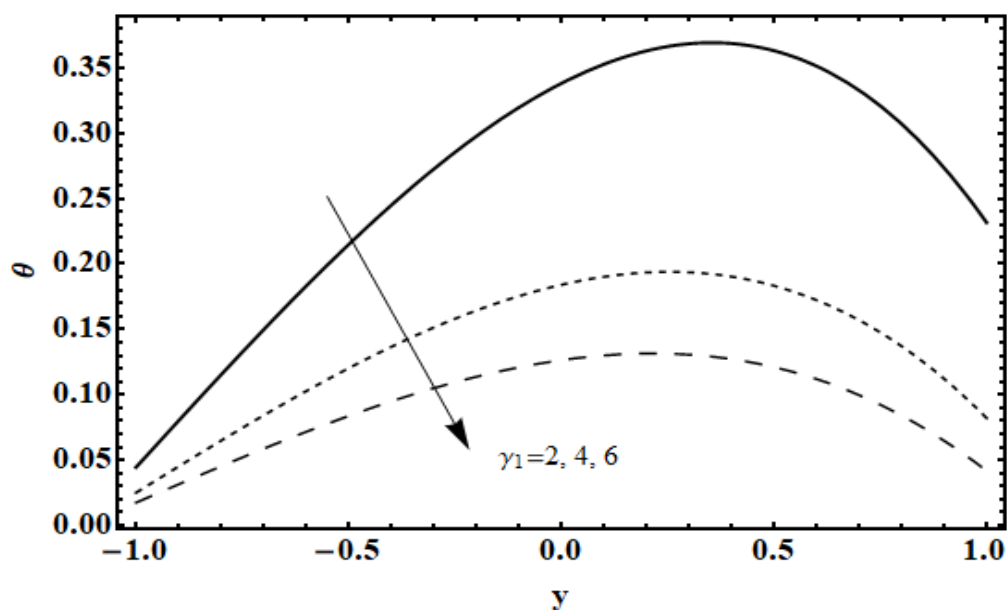


Fig 4.7 Plot of the temperature  $\theta$  for various values of the Biot number  $\gamma_1$ .

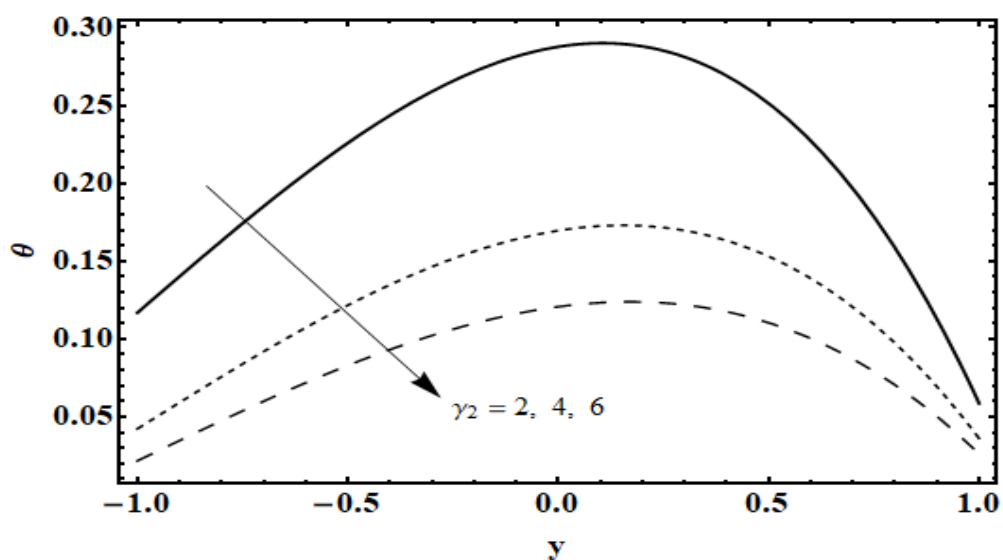


Fig 4.8 Plot of the temperature  $\theta$  for various values of the Biot number  $\gamma_2$ .

#### 4.4.2 Concentration profile

Figure 4.9 depicts the repercussion of the Dufour number  $Du$ . When the Dufour number rise in this case, the concentration drops.

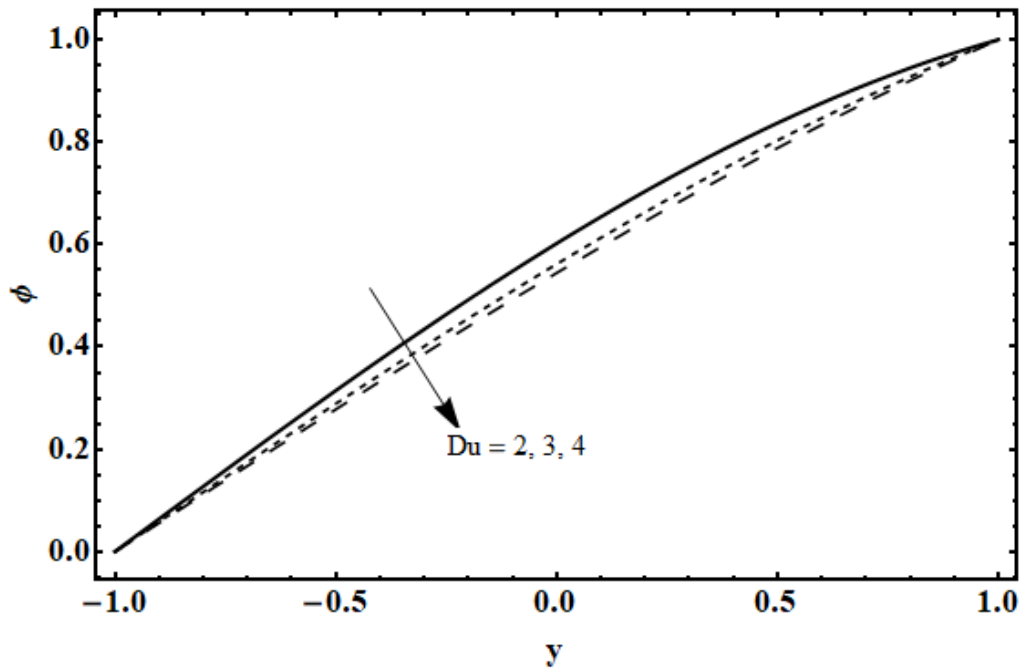


Fig 4.9 Plot of the concentration  $\phi$  for various values of the Dufour number  $Du$ .

The effects of the chemical reaction factor  $\gamma$  ( $\gamma > 0$  for destructive responses and  $\gamma < 0$  for generative responses) on the concentration profile are shown in Figure 4.10. It is observed that the spread of concentrations for destructive chemical changes is larger than those for generative actions. This is because generative chemical reactions cause the duration of chemical response to rise, which lowers the concentration profile.

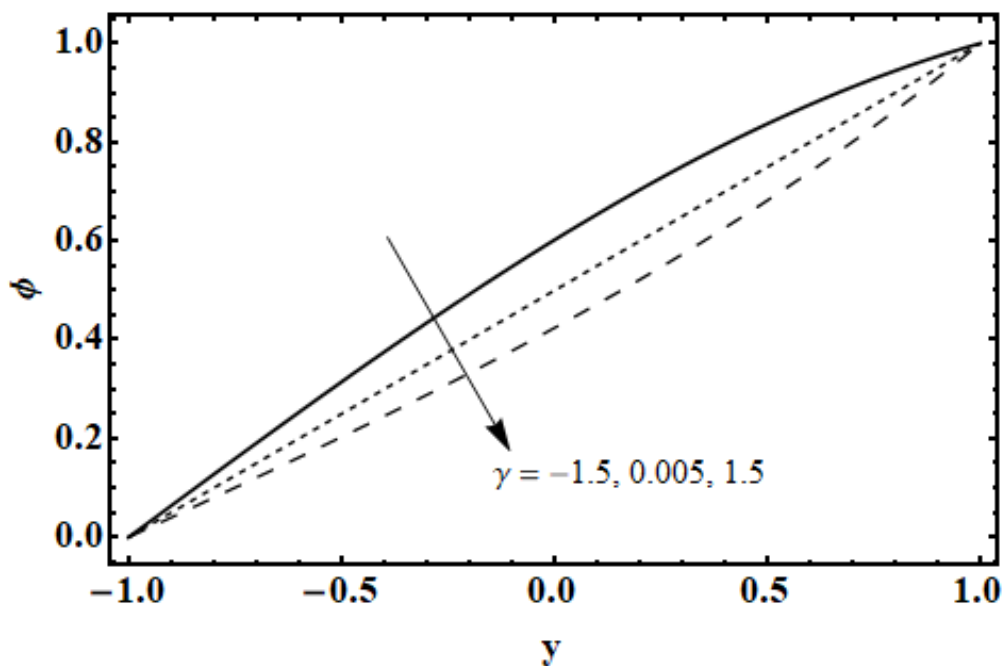


Fig 4.10 Plot of the concentration  $\phi$  for various values of the Chemical reaction parameter  $\gamma$ .

The concentration rises as the Schmidt value  $Sc$  rises because the molecular diffusion that drives intermolecular interactions between molecules diminishes as demonstrated in Figure 4.11.

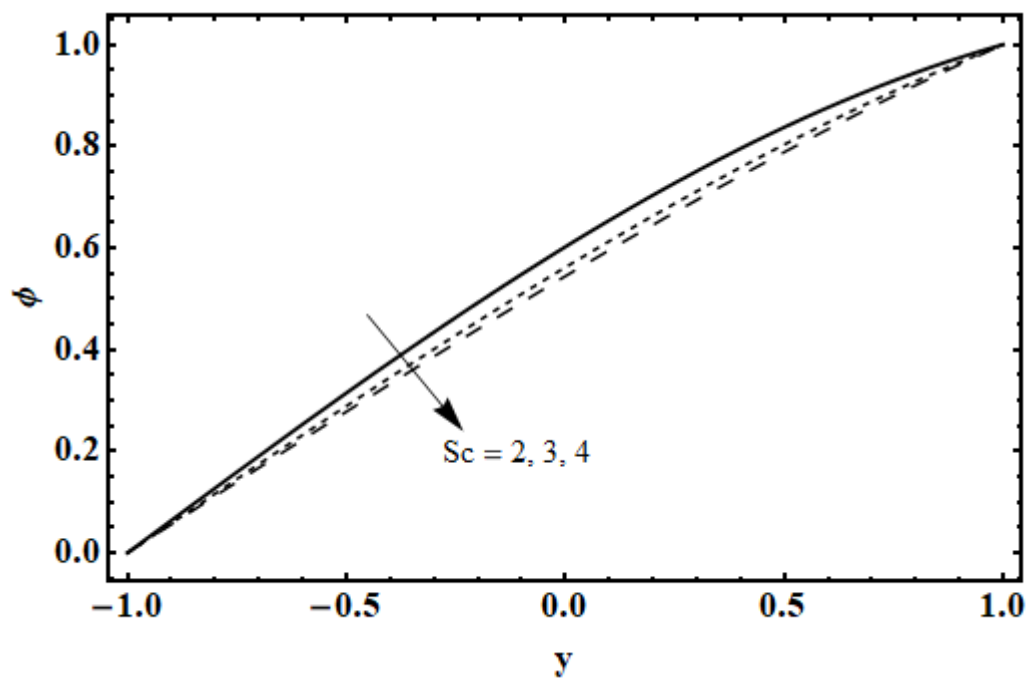
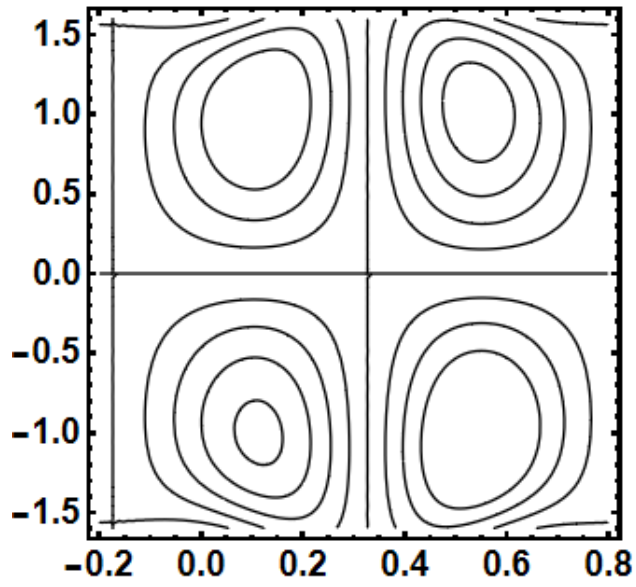


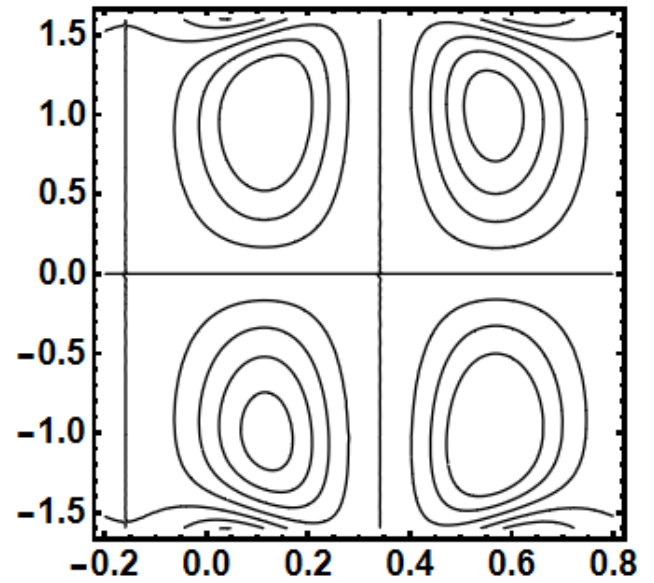
Fig 4.11 Plot of the concentration  $\phi$  for various values of the Schmidt number  $Sc$ .

### 4.4.3 Trapping

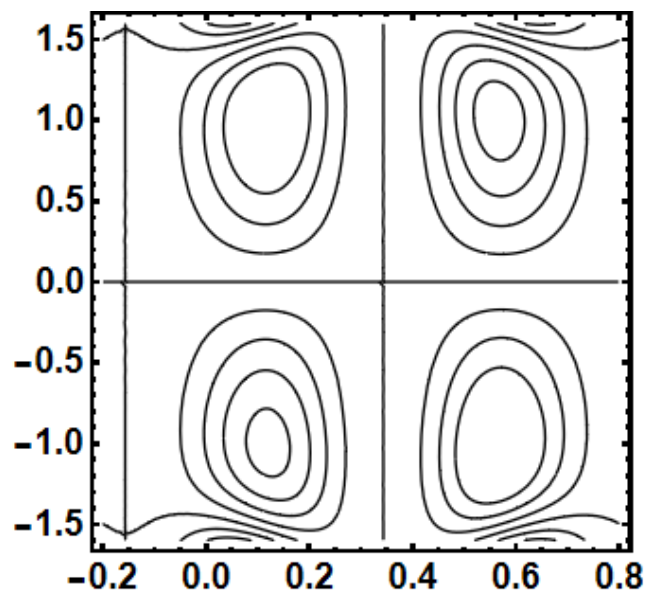
Closed and flowing streamlines are associated with trapping, an important fluid property. The peristaltic wave moves with the bolus, a closed internally circulating streamline. The production of a trapped bolus with variations in wall characteristics  $E_1$ ,  $E_2$ , and  $E_3$  is depicted in figures (4.12-4.14). The amount of the trapped bolus reduces as  $E_1$  increases, as seen in figure 4.12. Figure 4.13 demonstrate the decrease of bolus with  $E_2$  while figure 4.14 demonstrate that a rise in  $E_3$  has no discernible effect on the size of the bolus. The size of the trapped bolus decreases with increasing material fluid parameter  $K$ , as seen in figure 4.15. To investigate the behavior of fluid parameter  $M$ , figure 4.16 is plotted. The size of the trapped bolus decreases as  $M$  increases. Furthermore, the confined bolus resembles that of a viscous fluid when the Eyring-Powell fluid characteristics are absent.



(a)

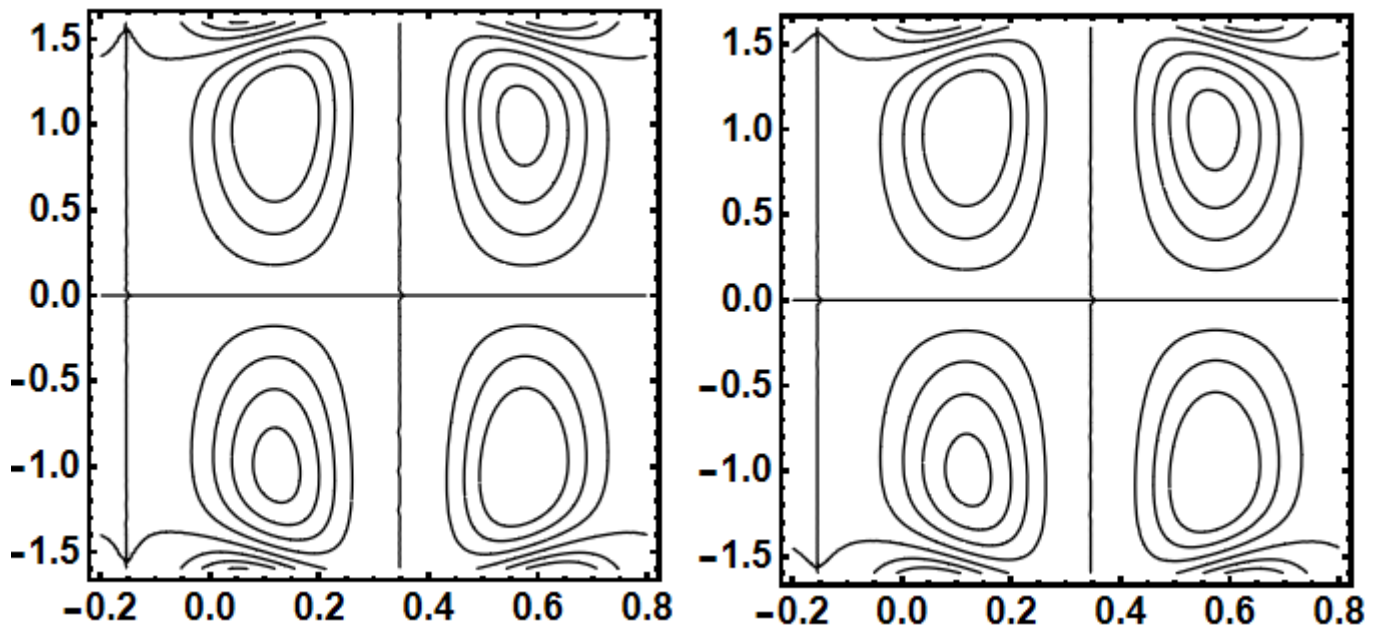


(b)



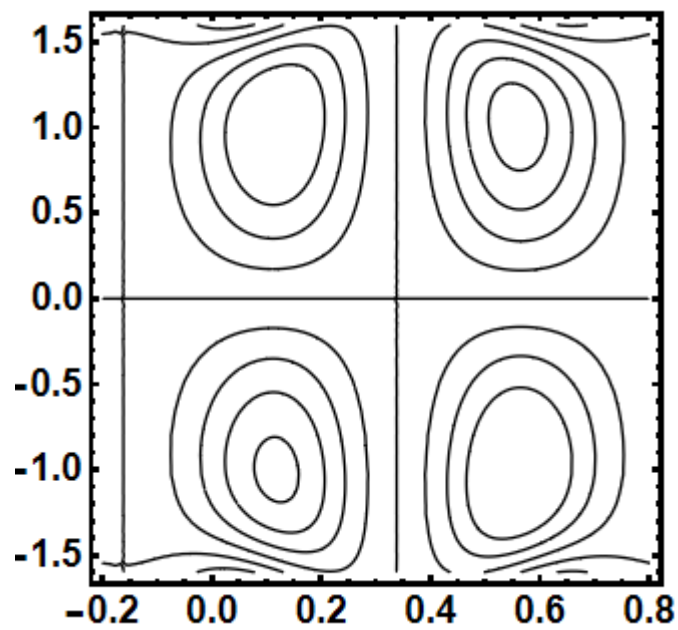
(c)

Fig 4.12 Effects of  $E_1$  on the streamline patterns of the fluid.



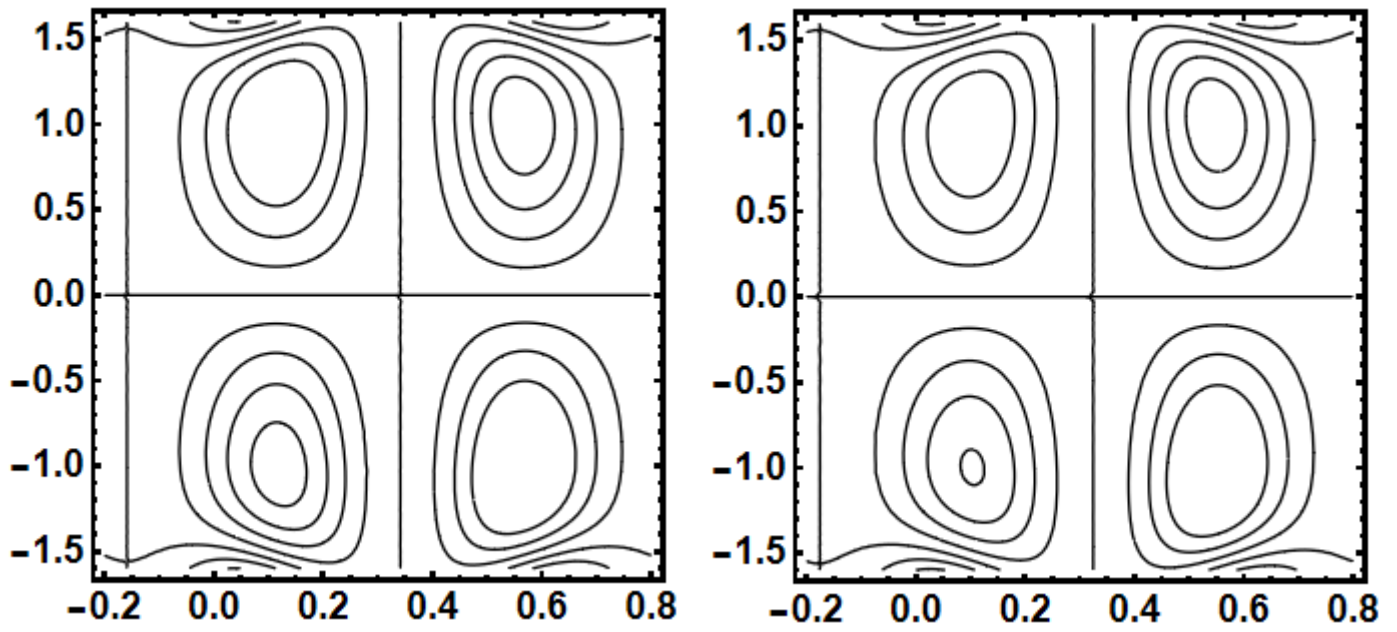
(a)

(b)



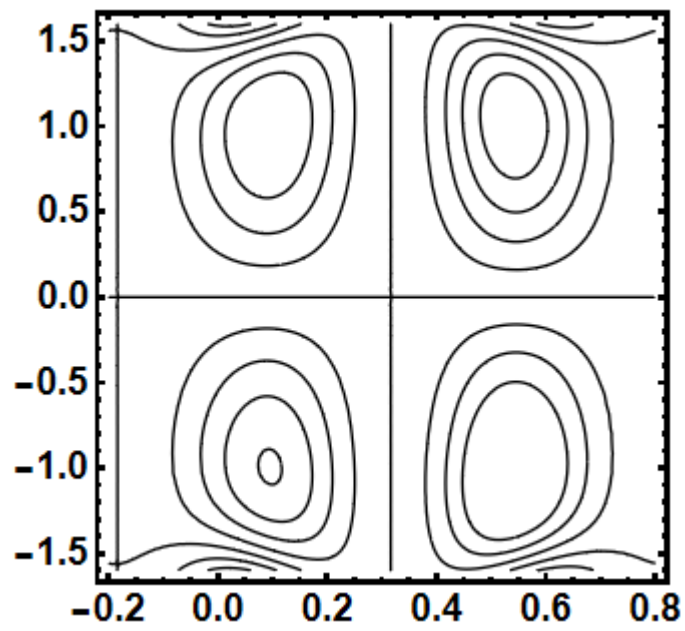
(c)

Fig 4.13 Effects of  $E_2$  on the streamline patterns of the fluid.



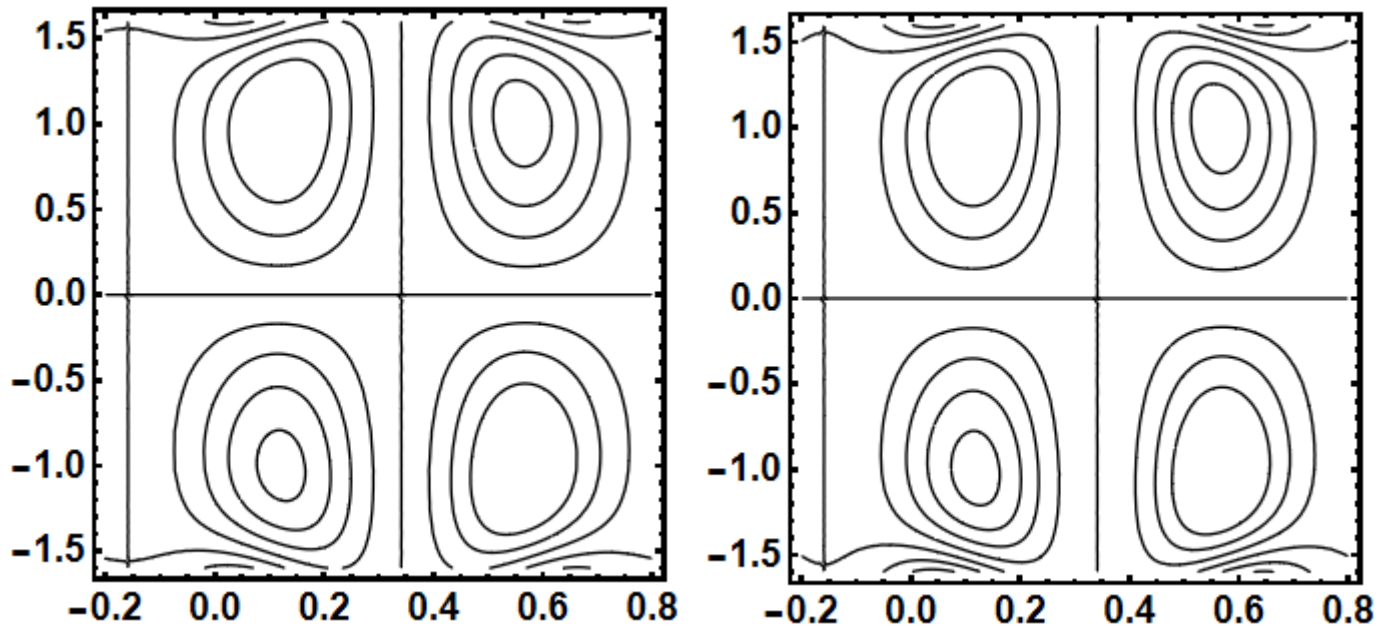
(a)

(b)



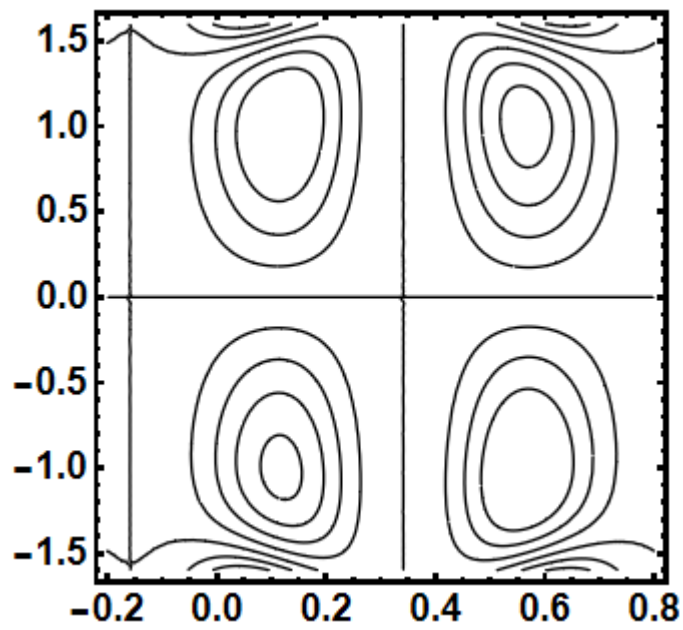
(c)

Fig 4.14 Effects of  $E_3$  on the streamline patterns of the fluid.



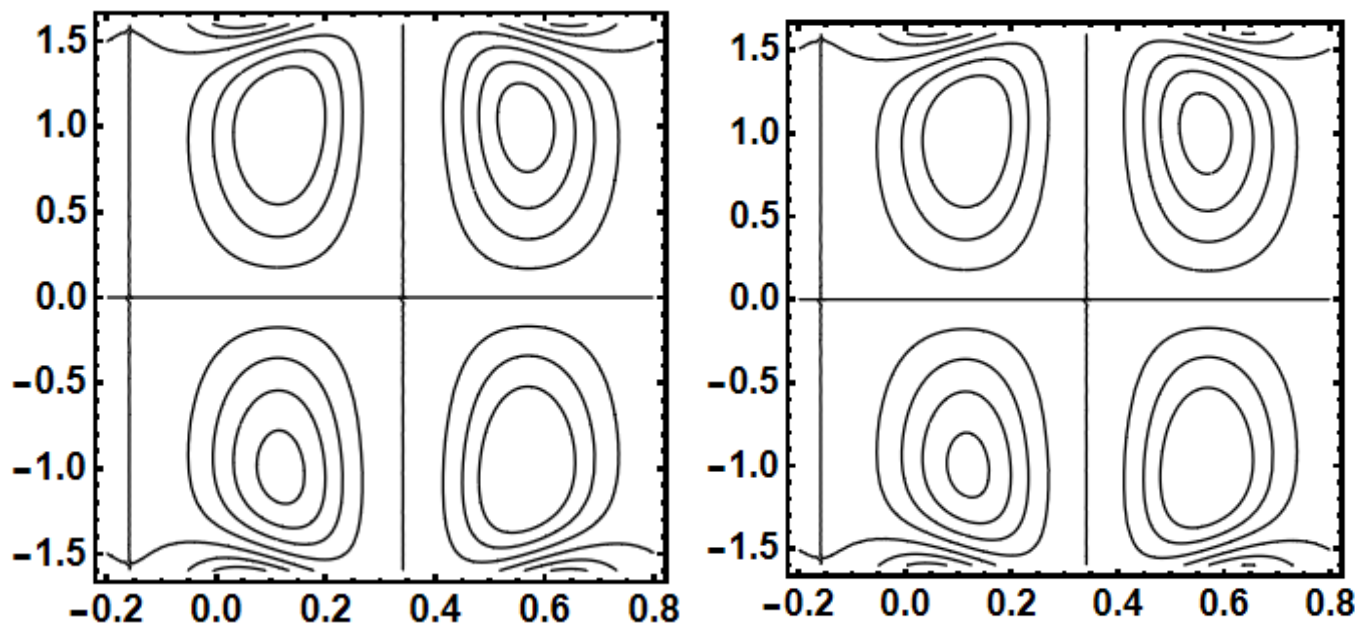
(a)

(b)



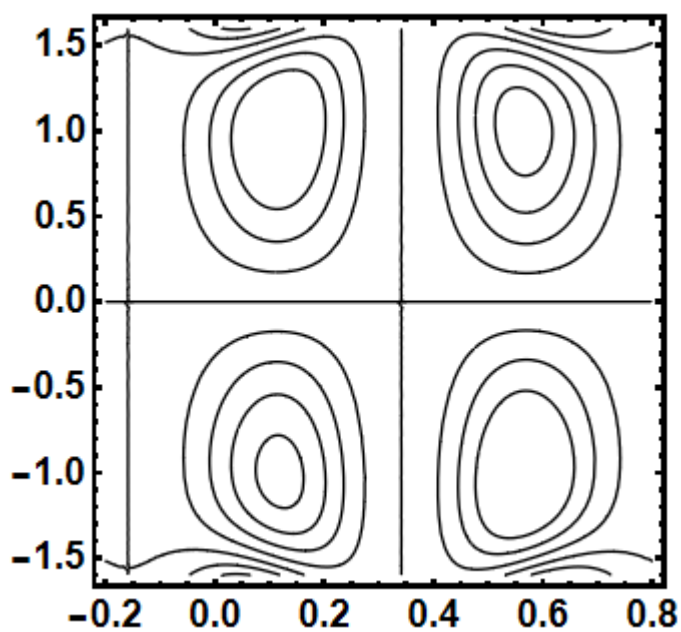
(c)

Fig 4.15 Effects of  $K$  on the streamline patterns of the fluid.



(a)

(b)



(c)

Fig 4.16 Effects of  $M$  on the streamline patterns of the fluid.

## 4.5 Concluding remarks

Here, we examined the Eyring-Powell liquid peristaltic circulation in a symmetric duct with flexible walls and convective circumstances. In an existence of Soret and Dufour numbers, evaluation has been conducted. The following is a list of major findings:

When the Eyring-Powell liquid factors,  $M$  and  $K$ , increase, the velocity field produces reverse outcomes. As the amounts of the Soret and Dufour factors increase, similar behavior is seen in the temperature and concentration curves. The temperature exhibits convection cooling close to the route walls as a function of Biot figures, which is falling. Additionally, the Biot factors affect the thermal transfer coefficient in two ways. As a specific instance of the current study, the specified surface temperature findings are inferred for  $\gamma_1 \rightarrow \infty$  and  $\gamma_2 \rightarrow \infty$ . A higher Schmidt value indicates a narrower temperature distribution and a more noticeable concentration profile. By raising the elasticity and Eyring-Powell fluid properties, the dimension of the trapped bolus reduces.

## CHAPTER 5

# CHARACTERISTICS OF PERISTALTIC FLOW OF WALTERS' B FLUID WITH CHEMICAL REACTION AND CONVECTIVE CONDITIONS

### 5.1 INTRODUCTION

In this chapter, motivated by the work of Hayat *et al.* [46] we have discussed the peristaltic movement of Walters' B fluid in an asymmetric porous channel. The equations have been quantitatively simulated using Mathematica. Furthermore, the perturbation approach to solve PDEs yielded the stream function's series solution.

### 5.2 MATHEMATICAL FORMULATION

To study the impact of viscous dissipation along with the chemical reaction on peristaltic Walters' B fluid in a porous asymmetric channel is considered. The walls of the geometry are defined in equation (5.1) and (5.2).

The geometry of the channel walls  $\widetilde{H}_1$  and  $\widetilde{H}_2$  is defined as:

$$\widetilde{H}_1(\widetilde{X}, \widetilde{t}) = d_1 + a_1 \sin\left[\frac{2\pi}{\lambda}(\widetilde{X} - c\widetilde{t})\right], \quad (5.1)$$

$$\widetilde{H}_2(\widetilde{X}, \widetilde{t}) = -d_2 - a_2 \sin\left[\frac{2\pi}{\lambda}(\widetilde{X} - c\widetilde{t}) + \phi\right]. \quad (5.2)$$

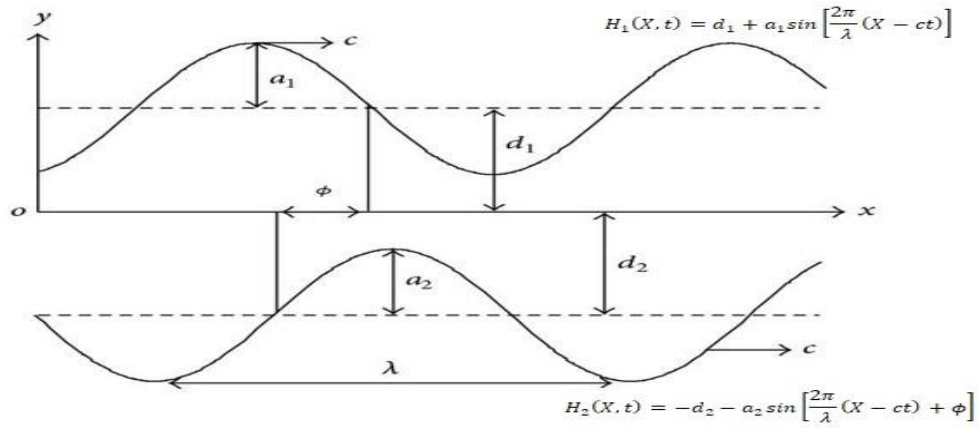


Figure 5.1 The geometry of the channel.

Here  $\lambda$  is the wavelength, ( $a_1$  and  $a_2$ ) is the amplitude, ( $d_1$  and  $d_2$ ) is the displacement,  $\phi$  is the phase velocity,  $c$  is the speed and  $\tilde{t}$  is the time.

The equations defining the suggested model are:

$$\nabla \cdot \tilde{\mathbf{V}} = 0, \quad (5.3)$$

$$\rho \frac{d\tilde{\mathbf{V}}}{d\tilde{t}} = -\nabla \tilde{P} + \nabla \cdot \tilde{\boldsymbol{\tau}} - \frac{\mu}{k_0} (\tilde{\mathbf{V}}), \quad (5.4)$$

where material time derivative ( $\frac{d}{d\tilde{t}}$ ), the velocity  $\tilde{\mathbf{V}} = (\tilde{u}, \tilde{v})$ ,  $\tilde{u}$  is in  $\tilde{x}$  direction and  $\tilde{v}$  is in  $\tilde{y}$  direction, density of liquid ( $\rho$ ), permeability parameter ( $k_0$ ), dynamic viscosity ( $\mu$ ) and extra stress tensor ( $\tilde{\boldsymbol{\tau}}$ ).

For Walters' B fluid, the extra stress tensor  $\tilde{\boldsymbol{\tau}}$  is given as:

$$\tilde{\tau} = 2\eta_0\tilde{e} - 2k_0\frac{\delta\tilde{e}}{\delta\tilde{t}}, \quad (5.5)$$

$$\frac{\delta\tilde{e}}{\delta\tilde{t}} = \frac{\partial\tilde{e}}{\partial\tilde{t}} + \tilde{V} \cdot \nabla\tilde{e} - \tilde{e} \cdot \nabla\tilde{V} - (\nabla\tilde{V})^T \cdot \tilde{e}, \quad (5.6)$$

$\eta_0$  and  $k_0$  are expressed as follows:

$$\eta_0 = \int_0^\infty N(\hat{t})d\hat{t}, \quad (5.7)$$

$$k_0 = \int_0^\infty \hat{t}N(\hat{t})d\hat{t}, \quad (5.8)$$

where the relaxation time is denoted by  $\hat{t}$ , and  $N(\hat{t})$  is the distribution function

$$\int_0^\infty \hat{t}^n N(\hat{t})d\hat{t}, \quad n \geq 2. \quad (5.9)$$

The following is the energy and mass equation:

$$\rho c_p \frac{d\tilde{T}}{d\tilde{t}} = k \nabla^2 \tilde{T} + \tilde{\tau}(\text{grad } \tilde{v}), \quad (5.10)$$

$$\frac{d\tilde{C}}{d\tilde{t}} = D \nabla^2 \tilde{C} - k_1(\tilde{C} - C_0), \quad (5.11)$$

where movement viscosity ( $\nu$ ), liquid humidity ( $\tilde{T}$ ), weight quantity ( $\tilde{C}$ ), lower border quantity ( $C_0$ ), the factor of weight diffusivity ( $D$ ), heat conductivity ( $k$ ), chemical response factor ( $k_1$ ),

extra stress tensor ( $\tilde{\tau}$ ) and  $\nabla^2 = (\frac{\partial^2}{\partial \tilde{x}^2} + \frac{\partial^2}{\partial \tilde{y}^2})$ .

The corresponding convective boundary conditions are:

$$\begin{aligned}
k \frac{\partial \tilde{T}}{\partial \tilde{Y}} &= -\eta_1 (\tilde{T} - \tilde{T}_1), & \text{at } \tilde{Y} = \tilde{H}_1, \\
k \frac{\partial \tilde{T}}{\partial \tilde{Y}} &= -\eta_2 (\tilde{T} - \tilde{T}_0), & \text{at } \tilde{Y} = \tilde{H}_2, \\
C &= 1 & \text{at } \tilde{Y} = \tilde{H}_1, \\
C &= 0 & \text{at } \tilde{Y} = \tilde{H}_2,
\end{aligned} \tag{5.12}$$

$\eta_1$  and  $\eta_2$  are heat transfer co-efficients.

Using the following transformation to transform the equations into steady frame and to perform the non-dimensional analysis, use the stream function and the non-dimensional quantities.

$$\begin{aligned}
x &= \tilde{X} - c\tilde{t}, \quad y = \tilde{Y}, \quad u = \tilde{U} - c, \quad v = \tilde{V}, \quad t^* = \tilde{T}, \quad u^* = \frac{\partial \tilde{\psi}}{\partial \tilde{y}}, \quad v^* = -\delta \frac{\partial \tilde{\psi}}{\partial \tilde{x}}, \\
\psi^* &= \frac{\tilde{\Psi}}{v}, \quad x^* = \frac{\tilde{x}}{\lambda}, \quad y^* = \frac{\tilde{y}}{d_1}, \quad \phi^* = \frac{\tilde{\phi}}{v}, \quad \delta = \frac{d}{\lambda}, \quad k = \frac{k_0 c}{\eta_0 d_1}, \quad \tau^* = \\
\frac{d_1}{\eta_0 c} \tau, \quad p^* &= \frac{d_1^2}{\eta_0 \lambda c} p, \quad Re = \frac{\rho c d_1}{\eta_0}, \quad h_1 = \frac{\tilde{H}_1}{d_1}, \quad h_2 = \frac{\tilde{H}_2}{d_1}.
\end{aligned} \tag{5.13}$$

$$\tilde{\tau}_{\tilde{x}\tilde{x}} = \eta_0 (4\tilde{u}_{\tilde{x}}) - k_0 (4\tilde{u}_{\tilde{x}\tilde{t}} + 4\tilde{u}_{\tilde{x}\tilde{x}} + 4\tilde{v}\tilde{u}_{\tilde{x}\tilde{y}} - 8\tilde{u}_{\tilde{x}}^2 - 4\tilde{v}_{\tilde{x}}\tilde{u}_{\tilde{y}} - 4\tilde{v}_{\tilde{x}}^2), \tag{5.14}$$

$$\begin{aligned}
\tilde{\tau}_{\tilde{x}\tilde{y}} &= \eta_0 (2\tilde{u}_{\tilde{y}} + 2\tilde{v}_{\tilde{x}}) - k_0 (2\tilde{u}_{\tilde{y}\tilde{t}} + 2\tilde{v}_{\tilde{x}\tilde{t}} + 2\tilde{u}\tilde{u}_{\tilde{x}\tilde{y}} + 2\tilde{u}\tilde{v}_{\tilde{x}\tilde{x}} + 2\tilde{v}\tilde{u}_{\tilde{y}\tilde{y}} + 2\tilde{v}\tilde{v}_{\tilde{x}\tilde{y}} - \\
&6\tilde{u}_{\tilde{x}}\tilde{u}_{\tilde{y}} - 2\tilde{u}_{\tilde{y}}\tilde{u}_{\tilde{y}} - 2\tilde{u}_{\tilde{x}}\tilde{u}_{\tilde{x}} - 6\tilde{v}_{\tilde{x}}\tilde{v}_{\tilde{y}}),
\end{aligned} \tag{5.15}$$

$$\tilde{\tau}_{\tilde{y}\tilde{y}} = \eta_0 (4\tilde{v}_{\tilde{y}}) - k_0 (4\tilde{u}_{\tilde{y}\tilde{t}} + 4\tilde{u}\tilde{u}_{\tilde{x}\tilde{y}} + 4\tilde{v}\tilde{v}_{\tilde{y}\tilde{y}} - 8\tilde{u}_{\tilde{y}}^2 - 4\tilde{v}\tilde{u}_{\tilde{y}} - 8\tilde{v}_{\tilde{y}}^2). \tag{5.16}$$

The equations for the fluid after using the transformation and dropping the star become:

$$\delta Re \left[ \left( \frac{\partial \psi}{\partial \tilde{y}} \frac{\partial}{\partial \tilde{x}} - \frac{\partial \psi}{\partial \tilde{x}} \frac{\partial}{\partial \tilde{y}} \right) \frac{\partial \psi}{\partial \tilde{y}} \right] = -\frac{\partial \rho}{\partial \tilde{x}} + \delta \frac{\partial \tilde{\tau}_{\tilde{x}\tilde{x}}}{\partial \tilde{x}} + \frac{\partial \tilde{\tau}_{\tilde{x}\tilde{y}}}{\partial \tilde{y}} - k \left( \frac{\partial \psi}{\partial \tilde{y}} + 1 \right), \quad (5.17)$$

$$-\delta^3 Re \left[ \left( \frac{\partial \psi}{\partial \tilde{y}} \frac{\partial}{\partial \tilde{x}} - \frac{\partial \psi}{\partial \tilde{x}} \frac{\partial}{\partial \tilde{y}} \right) \frac{\partial \psi}{\partial \tilde{x}} \right] = -\frac{\partial \rho}{\partial \tilde{y}} - \delta^2 \frac{\partial \tilde{\tau}_{\tilde{x}\tilde{y}}}{\partial \tilde{x}} - \delta \frac{\partial \tilde{\tau}_{\tilde{y}\tilde{y}}}{\partial \tilde{y}} + \delta^2 k \left( \frac{\partial \psi}{\partial \tilde{x}} \right), \quad (5.18)$$

$$\begin{aligned} \delta Re \left[ \left( \frac{\partial \psi}{\partial \tilde{y}} \frac{\partial}{\partial \tilde{x}} - \frac{\partial \psi}{\partial \tilde{x}} \frac{\partial}{\partial \tilde{y}} \right) \theta \right] &= \frac{1}{Pr} \left( \delta^2 \frac{\partial^2}{\partial \tilde{x}^2} + \frac{\partial^2}{\partial \tilde{y}^2} \right) \theta + Ec \left[ \delta \frac{\partial^2 \psi}{\partial \tilde{x} \partial \tilde{y}} (\tilde{\tau}_{\tilde{x}\tilde{x}} - \tilde{\tau}_{\tilde{y}\tilde{y}}) + \right. \\ &\left. \frac{\partial^2 \psi}{\partial \tilde{y}^2} \tilde{\tau}_{\tilde{x}\tilde{y}} - \delta^2 \frac{\partial^2 \psi}{\partial \tilde{x}^2} \tilde{\tau}_{\tilde{x}\tilde{y}} \right], \end{aligned} \quad (5.19)$$

$$\delta Re \left( \frac{\partial \psi}{\partial \tilde{y}} \frac{\partial \phi}{\partial \tilde{x}} - \frac{\partial \psi}{\partial \tilde{x}} \frac{\partial \phi}{\partial \tilde{y}} \right) = \frac{1}{Sr} \left( \delta^2 \frac{\partial^2 \phi}{\partial \tilde{x}^2} - \frac{\partial^2 \phi}{\partial \tilde{y}^2} \right) - \gamma \phi, \quad (5.20)$$

where  $Sr = \frac{v}{D}$ ,  $\gamma = \frac{k_1 d_1^2}{v}$ ,  $k = \frac{d_1^2}{k_1}$ .

By solving (5.17) and (5.18), we obtain the following compatibility equation for the fluid flow as:

$$\begin{aligned} \delta \left[ \frac{\partial}{\partial \tilde{y}} \left( \frac{\partial \tilde{\psi}}{\partial \tilde{y}} \frac{\partial^2 \tilde{\psi}}{\partial \tilde{x} \partial \tilde{y}} - \frac{\partial \tilde{\psi}}{\partial \tilde{x}} \frac{\partial^2 \tilde{\psi}}{\partial \tilde{y}^2} \right) + \delta^2 \frac{\partial}{\partial \tilde{x}} \left( \frac{\partial \tilde{\psi}}{\partial \tilde{y}} \frac{\partial^2 \tilde{\psi}}{\partial \tilde{x}^2} - \frac{\partial \tilde{\psi}}{\partial \tilde{x}} \frac{\partial^2 \tilde{\psi}}{\partial \tilde{x} \partial \tilde{y}} \right) \right] &= \delta \frac{\partial^2}{\partial \tilde{x} \partial \tilde{y}} (\tilde{S}_{\tilde{x}\tilde{x}} - \\ \tilde{S}_{\tilde{y}\tilde{y}}) + \left( \frac{\partial^2}{\partial \tilde{y}^2} - \delta^2 \frac{\partial^2}{\partial \tilde{x}^2} \right) \tilde{S}_{\tilde{x}\tilde{y}} \Big]. \end{aligned} \quad (5.21)$$

with boundary conditions:

$$\tilde{\Psi} = \frac{\tilde{F}}{2}, \quad \frac{\partial \tilde{\Psi}}{\partial \tilde{y}} = -1, \quad \frac{\partial \tilde{\theta}}{\partial \tilde{y}} + Bi_1 (\tilde{\theta} - 1) = 0, \quad \tilde{\theta} = 1,$$

$$\text{at } \tilde{y} = \tilde{h}_1(\tilde{x}) = 1 + a \sin(2\pi \tilde{x}),$$

$$\tilde{\Psi} = -\frac{\tilde{F}}{2}, \quad \frac{\partial \tilde{\Psi}}{\partial \tilde{y}} = -1, \quad \frac{\partial \tilde{\theta}}{\partial \tilde{y}} + Bi_2 (\tilde{\theta}) = 0, \quad \tilde{\theta} = 0,$$

$$\text{at } \tilde{y} = \tilde{h}_2(\tilde{x}) = -d - b\sin(2\pi\tilde{x} + \tilde{\theta}). \quad (5.22)$$

The dimensionless mean flow is denoted by  $Q$ , in the laboratory frame while in the wave frame, is denoted by  $F$ .

$$Q = F + I + d, \quad (5.23)$$

where  $F = \frac{q}{cd_1}$  with  $q = \int_{\tilde{h}_1(\tilde{x})}^{\tilde{h}_2(\tilde{x})} \tilde{u}(\tilde{x}, \tilde{y}) d\tilde{y}$ .

$$F = \int_{\tilde{h}_1(\tilde{x})}^{\tilde{h}_2(\tilde{x})} \frac{\partial \tilde{\psi}}{\partial \tilde{y}} d\tilde{y} = \tilde{\psi}(\tilde{h}_1(\tilde{x})) - \tilde{\psi}(\tilde{h}_2(\tilde{x})).$$

### 5.3 METHOD OF SOLUTION

The equation's solution is obtained by applying the perturbation method for small geometric parameters ( $\delta \ll 1$ ), taking into account the boundary condition.

$$\tilde{\psi} = \tilde{\psi}_0 + \delta\tilde{\psi}_1 + \delta^2\tilde{\psi}_2 + \dots, \quad (5.24)$$

$$\tilde{\theta} = \tilde{\theta}_0 + \delta\tilde{\theta}_1 + \delta^2\tilde{\theta}_2 + \dots, \quad (5.25)$$

$$\tilde{\theta} = \tilde{\theta}_0 + \delta\tilde{\theta}_1 + \delta^2\tilde{\theta}_2 + \dots, \quad (5.26)$$

$$\tilde{S}_{\tilde{x}\tilde{x}} = \tilde{S}_{0\tilde{x}\tilde{x}} + \delta\tilde{S}_{1\tilde{x}\tilde{x}} + \delta^2\tilde{S}_{2\tilde{x}\tilde{x}} + \dots, \quad (5.27)$$

$$\tilde{S}_{\tilde{y}\tilde{y}} = \tilde{S}_{0\tilde{y}\tilde{y}} + \delta\tilde{S}_{1\tilde{y}\tilde{y}} + \delta^2\tilde{S}_{2\tilde{y}\tilde{y}} + \dots, \quad (5.28)$$

$$\tilde{S}_{\tilde{x}\tilde{y}} = \tilde{S}_{0\tilde{x}\tilde{y}} + \delta\tilde{S}_{1\tilde{x}\tilde{y}} + \delta^2\tilde{S}_{2\tilde{x}\tilde{y}} + \dots, \quad (5.29)$$

$$\tilde{F} = \tilde{F}_0 + \delta \tilde{F}_1 + \delta^2 \tilde{F}_2 + \dots, \quad (5.30)$$

### 5.3.1 ZEROth ORDER SYSTEM

At the zeroth order, the resultant equation is provided by:

$$\frac{\partial^2}{\partial \tilde{y}^2} (S_{0\tilde{x}\tilde{y}}) - k \left( \frac{\partial^2 \tilde{\psi}_0}{\partial \tilde{y}^2} \right) = 0, \quad (5.31)$$

$$\frac{1}{Pr} \frac{\partial^2 \tilde{\theta}_0}{\partial \tilde{y}^2} + Ec \frac{\partial^2 \tilde{\psi}_0}{\partial \tilde{y}^2} (\tilde{S}_{0\tilde{x}\tilde{y}}) = 0, \quad (5.32)$$

$$\frac{1}{Sr} \frac{\partial^2 \tilde{\phi}_0}{\partial \tilde{y}^2} - \gamma \tilde{\phi}_0 = 0, \quad (5.33)$$

where  $S_{0\tilde{x}\tilde{y}} = 2 \frac{\partial^2 \tilde{\psi}_0}{\partial \tilde{y}^2},$

with boundary conditions:

$$\tilde{\Psi} = \frac{\tilde{F}}{2}, \quad \frac{\partial \tilde{\Psi}}{\partial \tilde{y}} = -1, \quad \frac{\partial \tilde{\theta}}{\partial \tilde{y}} + Bi_1(\tilde{\theta} - 1) = 0, \quad \tilde{\phi} = 1,$$

$$\text{at } \tilde{y} = \tilde{h}_1(\tilde{x}) = 1 + a \sin(2\pi \tilde{x}),$$

$$\tilde{\Psi} = -\frac{\tilde{F}}{2}, \quad \frac{\partial \tilde{\Psi}}{\partial \tilde{y}} = -1, \quad \frac{\partial \tilde{\theta}}{\partial \tilde{y}} + Bi_2(\tilde{\theta}) = 0, \quad \tilde{\phi} = 0,$$

$$\text{at } \tilde{y} = \tilde{h}_2(\tilde{x}) = -d - b \sin(2\pi \tilde{x} + \tilde{\phi}). \quad (5.34)$$

### 5.3.2 FIRST ORDER SYSTEM

The first order system of equation with boundary condition is given as follow:

$$Re \left[ \frac{\partial \tilde{\Psi}_0}{\partial \tilde{y}} \frac{\partial^3 \tilde{\Psi}_0}{\partial \tilde{x} \partial \tilde{y}^2} - \frac{\partial \tilde{\Psi}_0}{\partial \tilde{x}} \frac{\partial^3 \tilde{\Psi}_0}{\partial \tilde{y}^3} \right] = \frac{\partial^2}{\partial \tilde{y}^2} \tilde{S}_{1\tilde{x}\tilde{y}} + \frac{\partial^2}{\partial \tilde{x} \partial \tilde{y}} (\tilde{S}_{0\tilde{x}\tilde{x}} - \tilde{S}_{0\tilde{y}\tilde{y}}) - k \left( \frac{\partial^2 \tilde{\Psi}_1}{\partial \tilde{y}^2} \right), \quad (5.35)$$

$$\frac{1}{Pr} \frac{\partial^2 \tilde{\theta}_1}{\partial \tilde{y}^2} + Ec \left[ \frac{\partial^2 \tilde{\Psi}_0}{\partial \tilde{x} \partial \tilde{y}} (\tilde{S}_{0\tilde{x}\tilde{y}} - \tilde{S}_{0\tilde{y}\tilde{y}}) + \frac{\partial^2 \tilde{\Psi}_1}{\partial \tilde{y}^2} \tilde{S}_{1\tilde{x}\tilde{y}} \right] = Re \left[ \frac{\partial \tilde{\Psi}_0}{\partial \tilde{y}} \frac{\partial \tilde{\theta}_0}{\partial \tilde{x}} - \frac{\partial \tilde{\Psi}_0}{\partial \tilde{x}} \frac{\partial \tilde{\theta}_0}{\partial \tilde{y}} \right], \quad (5.36)$$

$$\frac{1}{Sr} \frac{\partial^2 \tilde{\phi}_1}{\partial \tilde{y}^2} - \gamma \tilde{\phi}_1 = 0. \quad (5.37)$$

with

$$\tilde{S}_{0\tilde{x}\tilde{x}} = 0, \quad \tilde{S}_{0\tilde{y}\tilde{y}} = 4k \left( \frac{\partial^2 \tilde{\Psi}_0}{\partial \tilde{y}^2} \right)^2,$$

$$\tilde{S}_{1\tilde{x}\tilde{y}} = 2 \left( \frac{\partial^2 \tilde{\Psi}_1}{\partial \tilde{y}^2} \right) - k \left[ -2 \frac{\partial^3 \tilde{\Psi}_0}{\partial \tilde{y}^3} \frac{\partial \tilde{\Psi}_0}{\partial \tilde{x}} - 4 \frac{\partial^2 \tilde{\Psi}_0}{\partial \tilde{x} \partial \tilde{y}} \frac{\partial^2 \tilde{\Psi}_0}{\partial \tilde{y}^2} + 2 \frac{\partial \tilde{\Psi}_0}{\partial \tilde{y}} \frac{\partial^3 \tilde{\Psi}_0}{\partial \tilde{x} \partial \tilde{y}^2} \right],$$

with boundary conditions:

$$\tilde{\Psi}_1 = \frac{\tilde{F}_1}{2}, \quad \frac{\partial \tilde{\Psi}_1}{\partial \tilde{y}} = 0, \quad \text{at } \tilde{y} = \tilde{h}_1(\tilde{x}) = 1 + \sin(2\pi\tilde{x}),$$

$$\frac{\partial \tilde{\theta}_1}{\partial \tilde{y}} + Bi_1 \tilde{\theta}_1 = 0, \quad \tilde{\phi}_1 = 0,$$

$$\tilde{\Psi}_1 = -\frac{\tilde{F}_1}{2}, \quad \frac{\partial \tilde{\Psi}_1}{\partial \tilde{y}} = 0, \quad \text{at } \tilde{y} = \tilde{h}_2(\tilde{x}) = -d - \sin(2\pi\tilde{x} + \tilde{\theta}),$$

$$\frac{\partial \tilde{\theta}_1}{\partial \tilde{y}} + Bi_2 \tilde{\theta}_1 = 0, \quad \tilde{\theta}_1 = 0. \quad (5.38)$$

The system of equations was solved by using Dsolve command in Mathematica. The graph for diverse parameters are also plotted by using the software.

#### 5.4 RESULTS AND DISCUSSION

The system of equations was solved by using Dsolve command in Mathematica. The graph for diverse parameters are also plotted by using the software.

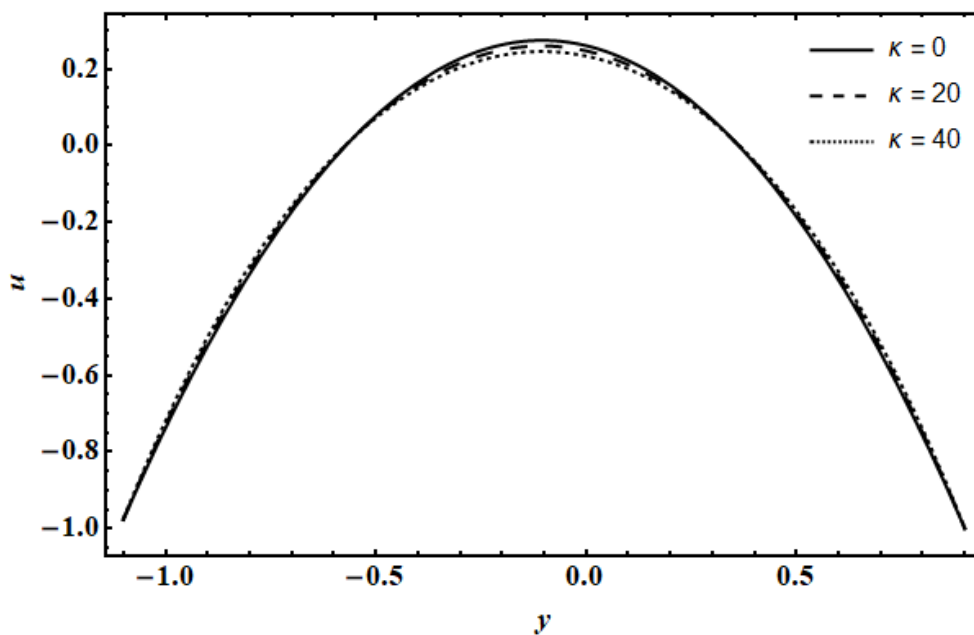


Fig 5.2 Impact of Walters' B Fluid parameter ( $\kappa$ ) on the velocity of the fluid.

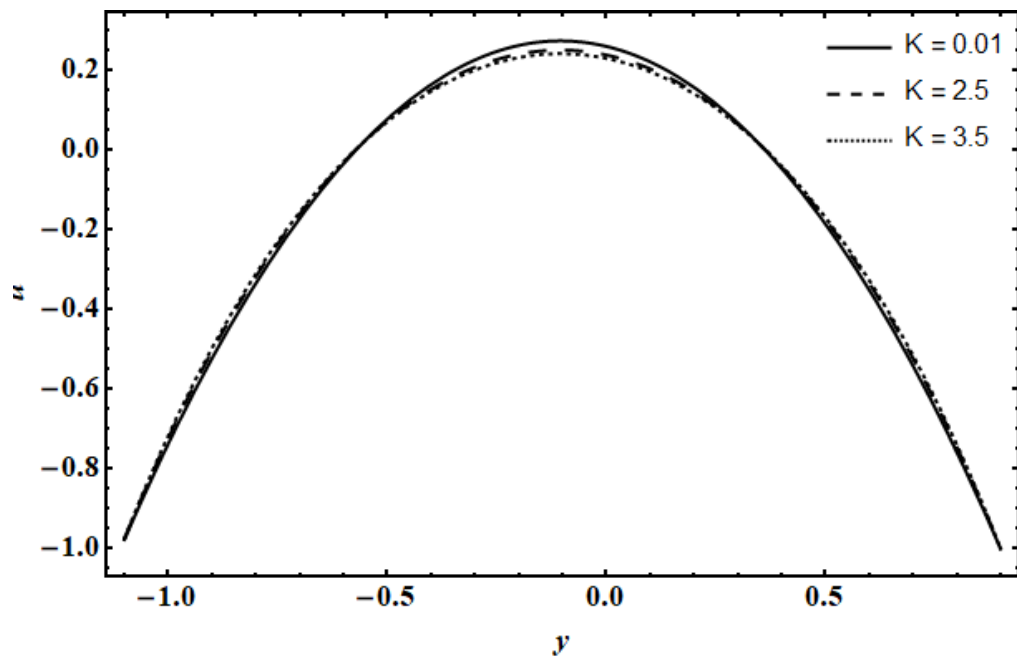


Fig 5.3 Impact of porosity parameter ( $K$ ) on the velocity of the fluid.

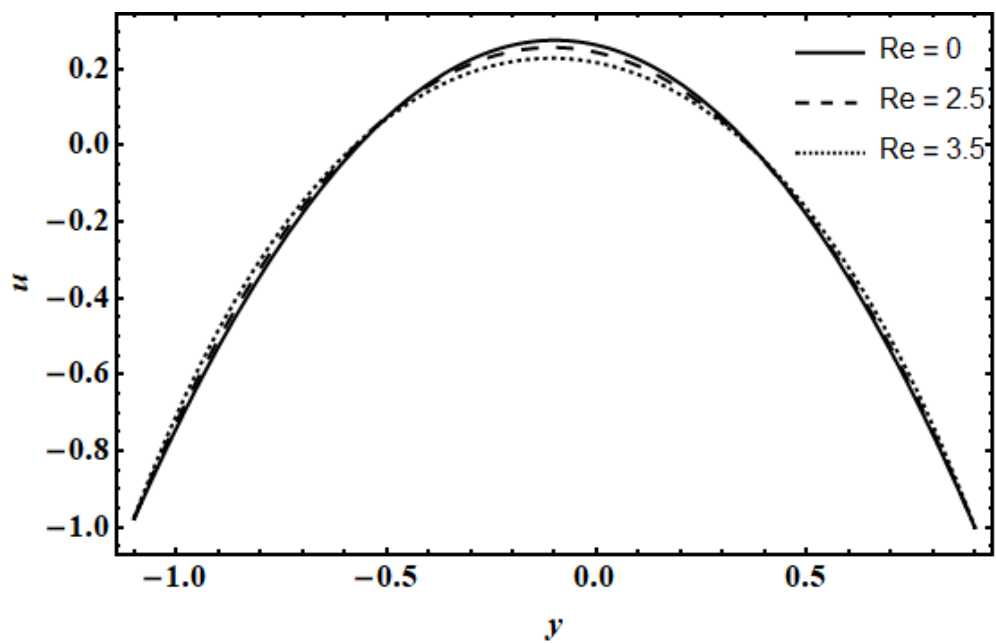


Fig 5.4 Impact of Reynolds number ( $Re$ ) on the velocity of the fluid.

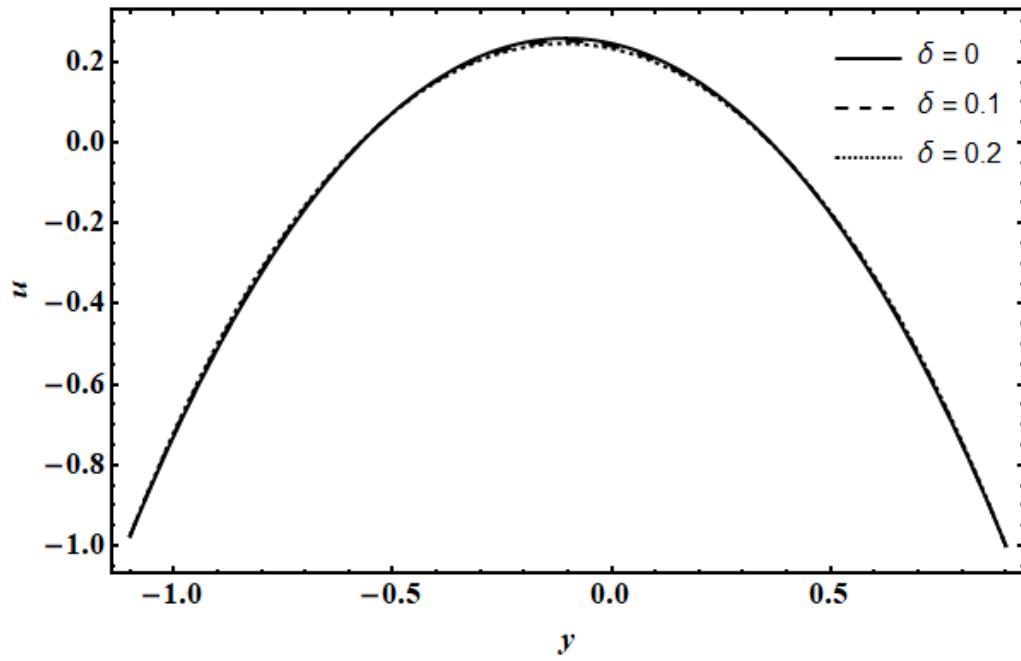


Fig 5.5 Impact of wavenumber ( $\delta$ ) on the velocity of the fluid.

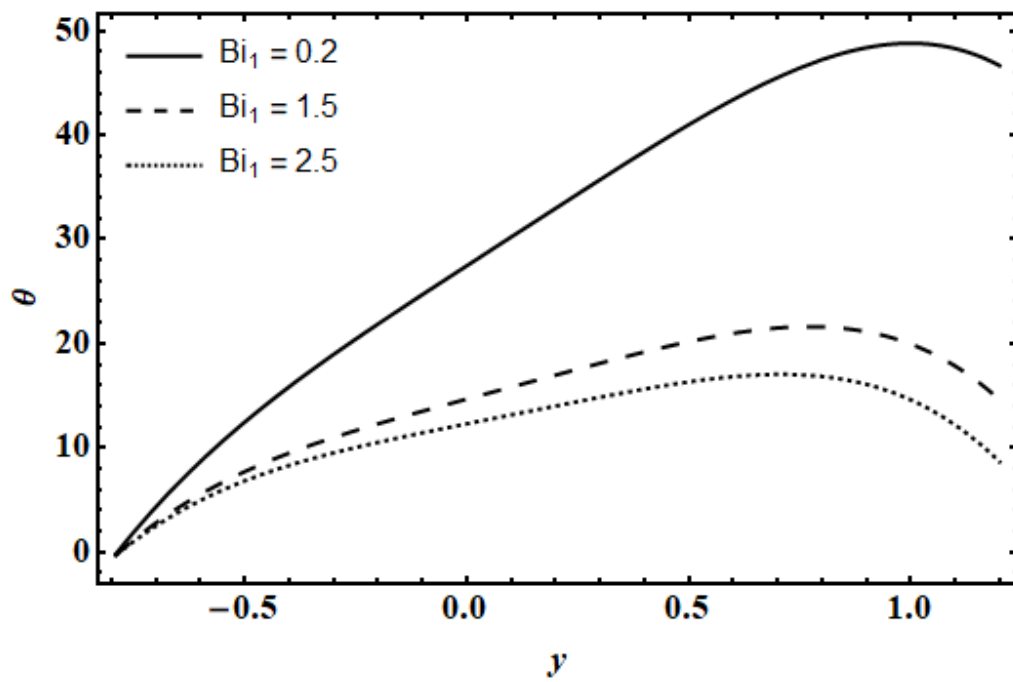
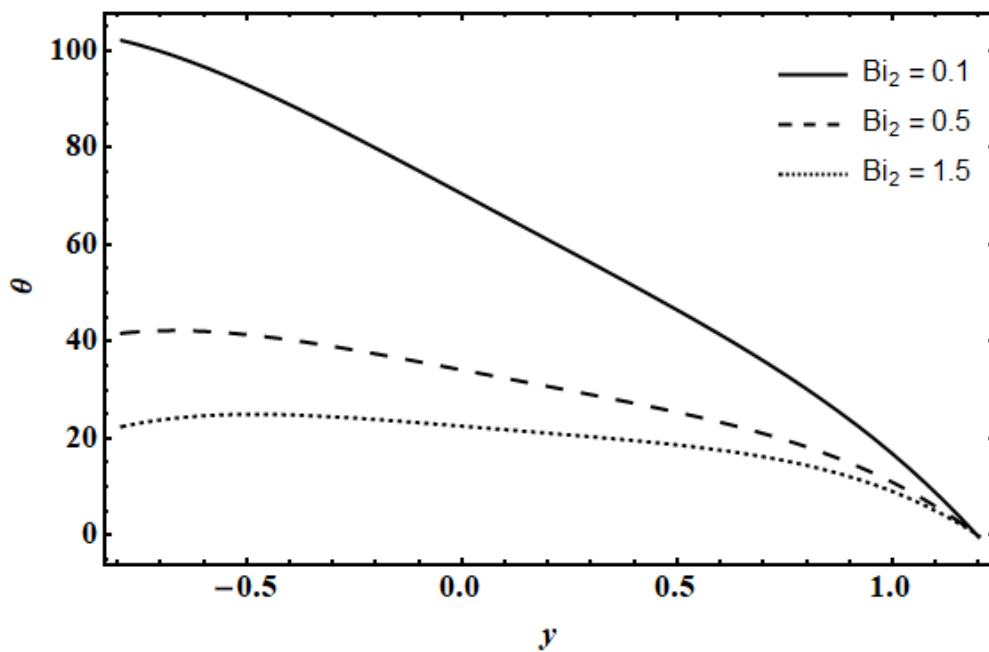
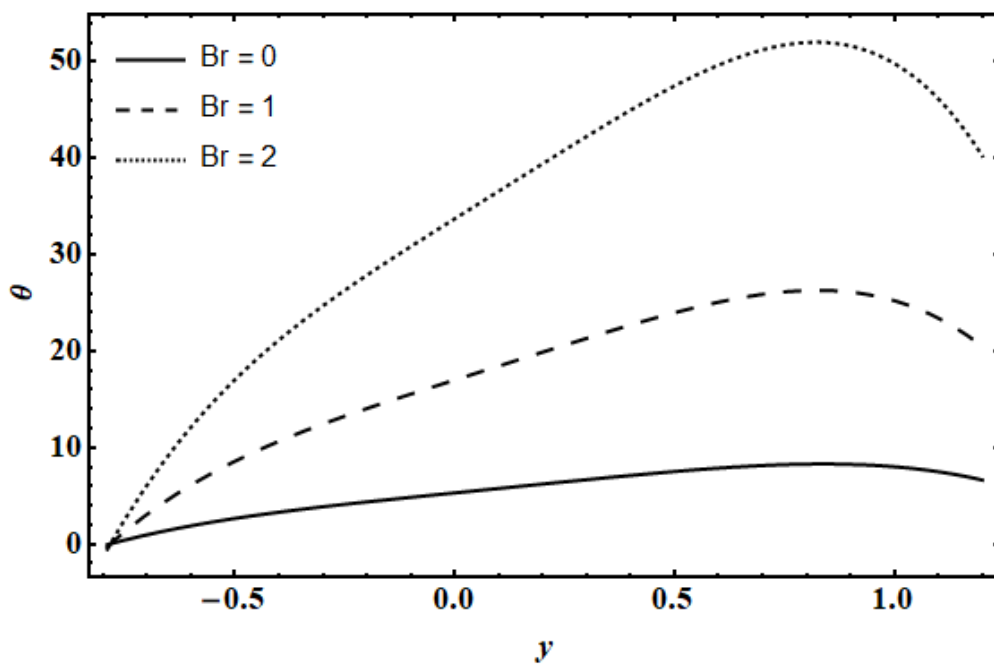


Fig 5.6 Temperature Profile for  $Bi_1$ .

Fig 5.7 Temperature Profile for  $Bi_2$ .Fig 5.8 Temperature Profile for  $Br$ .

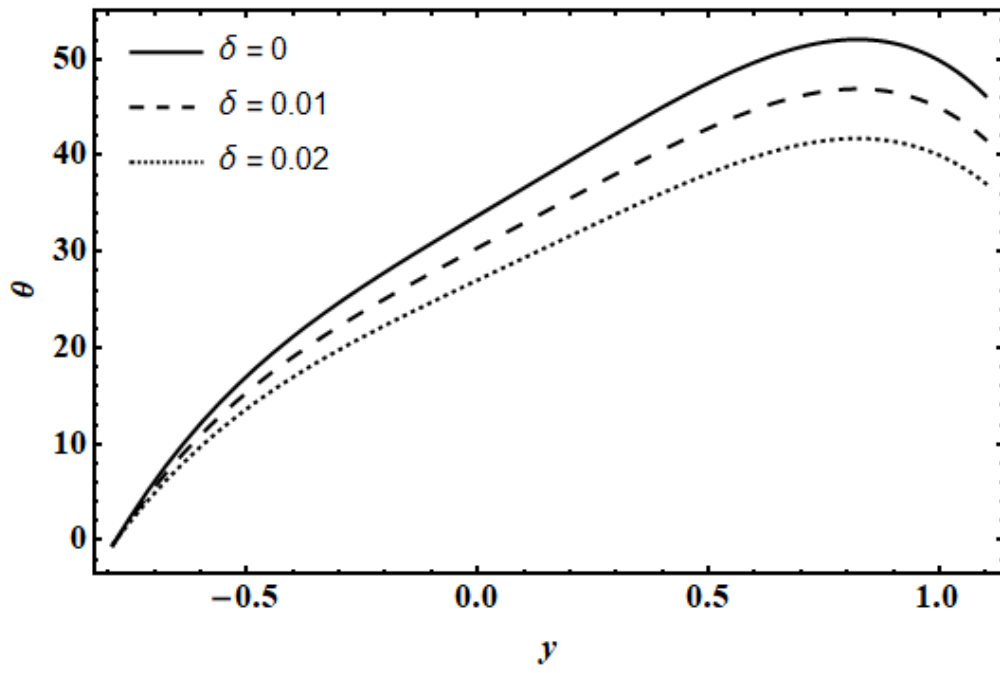


Fig 5.9 Temperature Profile for  $\delta$ .

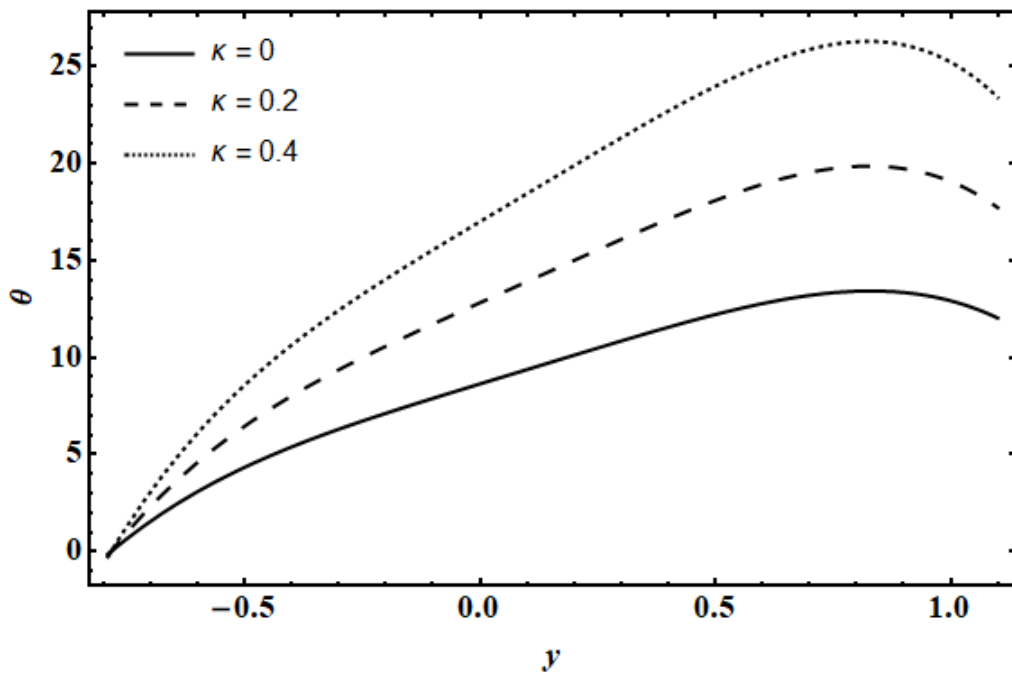


Fig 5.10 Temperature Profile for  $\kappa$ .

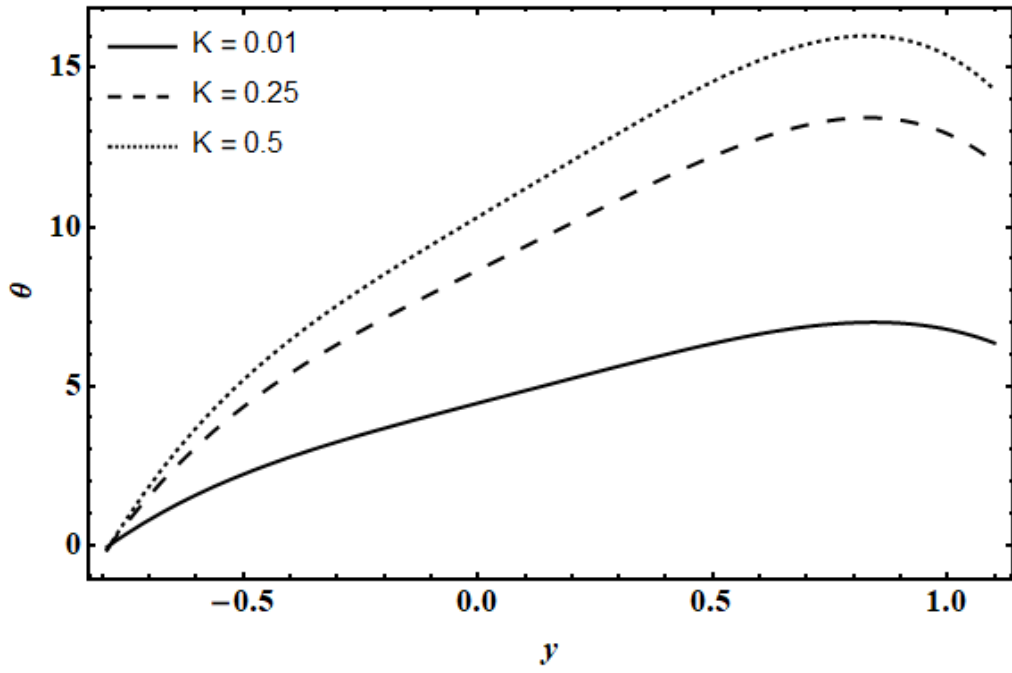


Fig 5.11 Temperature Profile for  $K$ .

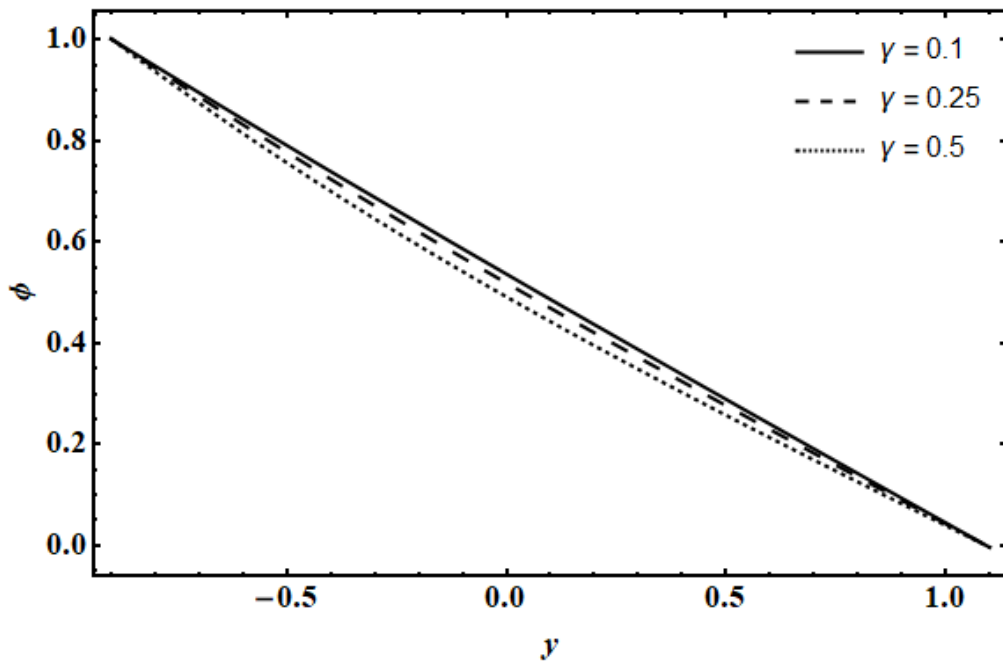


Fig 5.12 Concentration Profile for  $\gamma$ .

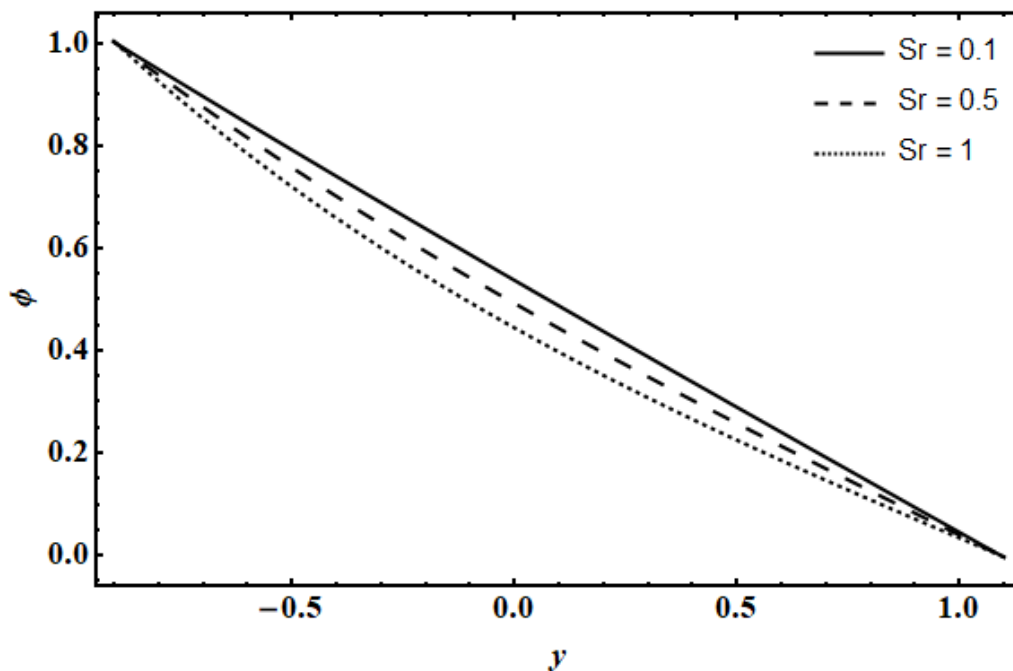


Fig 5.13 Concentration Profile for  $Sr$ .

In this section, the effect of physical parameters such as Walters' B fluid parameter, porosity parameter, Reynolds number, wavenumber, Soret number and chemical reaction parameter have been displayed in figures 5.2 – 5.13.

Figures 5.2 to 5.5 are prepared to discuss the variations of Walters' B fluid parameter, porosity parameter, Reynolds number and wavenumber on the velocity of the fluid. It can be perceived from Fig 5.2 that the velocity of the fluid lessens with the increase in  $\kappa$ . Increase in the value of porosity parameter  $K$  causes slightly decrease in the velocity profile as shown in Figure 5.3. Figure 5.4 investigate the effects of Reynolds numbers  $Re$  on the velocity profile. Graphical results indicate that with increase in the values of  $Re$  the velocity slightly decreases. It can be observed from Figure 5.5 that there is a slight change in the velocity of the fluid with the increase in the wave number  $\delta$ .

Figure 5.6 to 5.11 show the variations of Biot numbers  $Bi_1$  and  $Bi_2$ , Walters' B fluid parameter  $\kappa$ , Porosity parameter  $K$ , wavenumber  $\delta$  and Brinkmann number  $Br$  on the temperature profile. Effects of Biot numbers on the temperature profile are shown in the figures 5.6 and 5.7. The effects of Brinkmann number on the temperature profile are examined in Figure 5.8. The temperature increases along with the Brinkmann number value, according to the graph. Results obtained manifests decrease in temperature profile with increasing Biot numbers. Based on Figure 5.9, it is evident that the fluid's temperature decreases as the wave number  $\delta$  increases.

In figures 5.10 and 5.11 it is obvious that if the value of parameters increases causes the increase in temperature profile.

Figures 5.12 and 5.13 are plotted to study the effects of concentration profile for different values of  $\gamma$  and  $Sr$ . Figure 5.12 presents the consequences of chemical reaction parameter  $\gamma$  on concentration profile. It is seen that concentration distribution decreases with an increase in the value of chemical reaction. Effect of Soret number  $Sr$  is shown in the figure 5.13.

## CHAPTER 6

### CONCLUSION AND FUTURE WORK

#### 6.1 Conclusion

The research investigates the impact of MHD effects on the peristaltic motion of a Walters' B fluid within an asymmetric porous channel, accounting convective boundary conditions and chemical reaction. Utilizing a perturbation method, the study derives analytical expressions for the stream function.

In this study, the effect of convective boundary condition, MHD and chemical reactions on the peristaltic flow of Walters' B fluid in an asymmetric channel has been investigated. Using appropriate similarity transformations, the system of partial differential equations is first expressed in terms of ordinary differential equations, and it is then analytically solved using the perturbation method. Specifically, analytical solutions for temperature, concentration, and velocity have been provided. Graphs are used to discuss the results. The main observation in this study are:

The value of velocity decreases as the value of parameters ( $\kappa$  and  $K$ ), wave number  $\delta$  and Reynolds number is increases. The temperature decreases with an increase in Biot numbers ( $Bi_1$  and  $Bi_2$ ) and wave number  $\delta$  while with increase in  $\kappa$ ,  $Br$  and  $K$ , the temperature increases. With the increase in  $\gamma$  and  $Sr$ , the concentration decreases.

### **6.3 Future work**

This work may further be extended by adding more bodies forces to the model, like MHD, inclined magnetic field, double diffusion, etc. The entropy generation can also be discussed as it's extension. Impact of nonlinear thermal radiation can also be discussed. The consequences of Walters' B fluid can also be discussed in various geometries, such as ducts, curved channels, symmetrical structures, etc.

## REFERENCES

1. Latham, T. W. (1966). Fluid motions in a peristaltic pump (*Doctoral dissertation, Massachusetts Institute of Technology*).
2. Siddiqui, A. M., & Schwarz, W. H. (1994). Peristaltic flow of a second-order fluid in tubes. *Journal of Non-Newtonian Fluid Mechanics*, 53, 257-284.
3. Akhtar, S., Almutairi, S., & Nadeem, S. (2022). Impact of heat and mass transfer on the Peristaltic flow of non-Newtonian Casson fluid inside an elliptic conduit: Exact solutions through novel technique. *Chinese Journal of Physics*, 78, 194-206.
4. Nadeem, S., Akbar, N. S., Bibi, N., & Ashiq, S. (2010). Influence of heat and mass transfer on peristaltic flow of a third order fluid in a diverging tube. *Communications in Nonlinear Science and Numerical Simulation*, 15(10), 2916-2931.
5. Ellahi, R., Bhatti, M. M., & Vafai, K. (2014). Effects of heat and mass transfer on peristaltic flow in a non-uniform rectangular duct. *International Journal of Heat and Mass Transfer*, 71, 706-719.
6. Mehmood, O. U., Qureshi, A. A., Yasmin, H., & Uddin, S. (2020). Thermo-mechanical analysis of non Newtonian peristaltic mechanism: Modified heat flux model. *Physica A: Statistical Mechanics and its Applications*, 550, 124014.
7. Zeeshan, A., Riaz, A., Alzahrani, F., & Moqeet, A. (2022). Flow analysis of two-layer Nano/Johnson–Segalman fluid in a blood vessel-like tube with complex peristaltic wave. *Mathematical Problems in Engineering*, 2022, 1-18.
8. Tripathi, D., Sharma, A., & Bég, O. A. (2018). Joule heating and buoyancy effects in electro-osmotic peristaltic transport of aqueous nanofluids through a microchannel with complex wave propagation. *Advanced Powder Technology*, 29(3), 639-653.
9. Javid, K., Ali, N., & Asghar, Z. (2019). Numerical simulation of the peristaltic motion of a viscous fluid through a complex wavy non-uniform channel with magnetohydrodynamic effects. *Physica Scripta*, 94(11), 115226.
10. Tripathi, D., Jhorar, R., Bég, O. A., & Kadir, A. (2017). Electro-magneto-hydrodynamic peristaltic pumping of couple stress biofluids through a complex wavy micro-channel. *Journal of Molecular Liquids*, 236, 358-367.
11. Bhatti, M. M., Ellahi, R., Zeeshan, A., Marin, M., & Ijaz, N. (2019). Numerical study of heat transfer and Hall current impact on peristaltic propulsion of particle-fluid suspension with compliant wall properties. *Modern Physics Letters B*, 33(35), 1950439.
12. Ali, N., Hussain, S., & Ullah, K. (2020). Theoretical analysis of two-layered electro-osmotic peristaltic flow of FENE-P fluid in an axisymmetric tube. *Physics of Fluids*, 32(2).
13. Ali, N., Hussain, S., Ullah, K., & Bég, O. A. (2019). Mathematical modelling of two-fluid electro-osmotic peristaltic pumping of an Ellis fluid in an axisymmetric tube. *The European Physical Journal Plus*, 134(4), 141.
14. Prakash, J., Tripathi, D., Tiwari, A. K., Sait, S. M., & Ellahi, R. (2019). Peristaltic pumping of nanofluids through a tapered channel in a porous environment: applications in blood flow. *Symmetry*, 11(7), 868.

15. Mansour, H. M., & Abou-zeid, M. Y. (2019). Heat and mass transfer effect on non-Newtonian fluid flow in a non-uniform vertical tube with peristalsis. *Journal of Advanced Research in Fluid Mechanics and Thermal Sciences*, 61(1), 44-62.
16. Fung, Y. C., & Yih, C. S. (1968). Peristaltic transport. *J. Appl. Mech.*
17. Tripathi, D. (2011). Peristaltic transport of a viscoelastic fluid in a channel. *Acta Astronautica*, 68(7-8), 1379-1385.
18. Baliga, D., Gudekote, M., Choudhari, R., Vaidya, H., & Prasad, K. V. (2019). Influence of velocity and thermal slip on the peristaltic transport of a herschel-bulkley fluid through an inclined porous tube. *Journal of Advanced Research in Fluid Mechanics and Thermal Sciences*, 56(2), 195-210.
19. Rajashekhar, C., Mebarek-Oudina, F., Vaidya, H., Prasad, K. V., Manjunatha, G., & Balachandra, H. (2021). Mass and heat transport impact on the peristaltic flow of a Ree–Eyring liquid through variable properties for hemodynamic flow. *Heat Transfer*, 50(5), 5106-5122.
20. Saleem, A., Akhtar, S., Alharbi, F. M., Nadeem, S., Ghalambaz, M., & Issakhov, A. (2020). Physical aspects of peristaltic flow of hybrid nano fluid inside a curved tube having ciliated wall. *Results in Physics*, 19, 103431.
21. Rafiq, M., Shaheen, A., Trabelsi, Y., Eldin, S. M., Khan, M. I., & Suker, D. K. (2023). Impact of activation energy and variable properties on peristaltic flow through porous wall channel. *Scientific Reports*, 13(1), 3219.
22. Abbasi, A., Khan, S. U., Farooq, W., Mughal, F. M., Khan, M. I., Prasannakumara, B. C., ... & Galal, A. M. (2023). Peristaltic flow of chemically reactive Ellis fluid through an asymmetric channel: Heat and mass transfer analysis. *Ain Shams Engineering Journal*, 14(1), 101832.
23. Sushma M Puranik, Indira Rama Rao, K.R. Sreegowray, Fehmi Gamaoun, Umair Khan, Sayed M.Eldin , Konduru Sarada , Jasgurpreet Singh Chohan , Abdulkafi Mohammed Saeed. "Effect of heat transfer on peristaltic flow of Newtonian fluid through eccentric cylinders." *Case Studies in Thermal Engineering*, Volume 45, May 2023, 102912.
24. Nazeer, M., Irfan, M., Hussain, F., Siddique, I., Khan, M. I., Guedri, K., & Galal, A. M. (2023). Analytical study of heat transfer rate of peristaltic flow in asymmetric channel with laser and magnetic effects: remedy for autoimmune disease. *International Journal of Modern Physics B*, 37(03), 2350025.
25. Rafiq, M., Shaheen, S., Khan, M. I., Fadhl, B. M., Hassine, S. B. H., & Eldin, S. M. (2023). Impact of ciliated walls on peristaltic flow of Rabinowitsch fluid through flexible tube with heat/mass transfer. *Case Studies in Thermal Engineering*, 45, 102990.
26. Alhazmi, S.E., Imran, A., Awais, M. *et al.* Thermal convection in nanofluids for peristaltic flow in a nonuniform channel. *Sci Rep* 12, 12656 (2022).
27. Vaidya, H., Prasad, K. V., Khan, M. I., Mebarek-Oudina, F., Tlili, I., Rajashekhar, C., ... & Al-Gamdi, S. G. (2022). Combined effects of chemical reaction and variable thermal conductivity on MHD peristaltic flow of Phan-Thien-Tanner liquid through inclined channel. *Case Studies in Thermal Engineering*, 36, 102214.
28. Ibrahim, M. G., & Abou-Zeid, M. Y. (2022). Influence of variable velocity slip condition and activation energy on MHD peristaltic flow of Prandtl nanofluid through a non-uniform channel. *Scientific Reports*, 12(1), 18747.
29. Arafa, A. A., Ahmed, S. E., & Allan, M. M. (2022). Peristaltic flow of non-homogeneous nanofluids through variable porosity and heat generating porous media with viscous dissipation: Entropy analyses. *Case Studies in Thermal Engineering*, 32, 101882.

30. Qureshi, I. H., Awais, M., Awan, S. E., Abrar, M. N., Raja, M. A. Z., Alharbi, S. O., & Khan, I. (2021). Influence of radially magnetic field properties in a peristaltic flow with internal heat generation: Numerical treatment. *Case Studies in Thermal Engineering*, 26, 101019.
31. Walters, K. J. (1962). Non-Newtonian effects in some elastico-viscous liquids whose behaviour at small rates of shear is characterized by a general linear equation of state. *The Quarterly Journal of Mechanics and Applied Mathematics*, 15(1), 63-76.
32. Makinde, O. D., Gnanewara Reddy, M., & Venugopal Reddy, K. (2017). Effects of thermal radiation on MHD peristaltic motion of Walters-B fluid with heat source and slip conditions. *Journal of Applied Fluid Mechanics*, 10(4), 1105-1112.
33. Nandeppanavar, M. M., Abel, M. S., & Tawade, J. (2010). Heat transfer in a Walter's liquid B fluid over an impermeable stretching sheet with non-uniform heat source/sink and elastic deformation. *Communications in Nonlinear Science and Numerical Simulation*, 15(7), 1791-1802.
34. Siddique, I., Shah, N. A., & Abro, K. A. (2021). Thermography of ferromagnetic Walter's-B fluid through varying thermal stratification. *South African Journal of Chemical Engineering*, 36, 118-126.
35. Yu-MingChu Mujeebur Rahman M.Ijaz Khan SeifedineKadry WasifUr Rehman ZahraAbdelmalek. Heat transport and bio-convective nanomaterial flow of Walter's-B fluid containing gyrotactic microorganisms, *Ain Shams Engineering Journal*, Volume 12, Issue 3, September 2021, Pages 3071-3079.
36. Tanveer, A., Khan, M., Salahuddin, T., Al Alwan, B., & Amari, A. (2022). Dynamics of Walters' B fluid due to periodic wave in a convectively heated channel with internal heat generation. *Mathematics and Computers in Simulation*, 199, 374-393.
37. Thawi, M., & Hummady, L. (2023). Impact of Couple Stress with Rotation on Walters, B Fluid in Porous Medium. *Iraqi Journal For Computer Science and Mathematics*, 4(2), 189-201.
38. Jaafar, Z. A., Hummady, L. Z., & Thawi, M. H. (2023). Influence of some fluid mechanic parameters caused from heat transport with rotation on Walters' B fluid. *Journal of Biomechanical Science and Engineering Japan Society of Mechanical Engineers ISSN: 1880-9863 New Normal in the Field of Nursing, Medicine, Management, Technology DOI 10.17605/OSF.IO/TYRMA*.
39. Alfvén, H. (1942). Existence of electromagnetic-hydrodynamic waves. *Nature*, 150(3805), 405-406.
40. Mallikarjuna, B., Bhatta, S. S., & Ramprasad, S. (2021). Velocity and thermal slip effects on MHD convective radiative two-phase flows in an asymmetric non-uniform channel. *Propulsion and Power Research*, 10(2), 169-179.
41. Ali, N., Hussain, Q., Hayat, T., & Asghar, S. (2008). Slip effects on the peristaltic transport of MHD fluid with variable viscosity. *Physics Letters A*, 372(9), 1477-1489.
42. Machireddy, G. R., & Kattamreddy, V. R. (2016). Impact of velocity slip and joule heating on MHD peristaltic flow through a porous medium with chemical reaction. *Journal of the Nigerian Mathematical society*, 35(1), 227-244.
43. El-dabe, N. T., & Mostapha, D. R. (2019). MHD peristaltic flow of a Walters' B fluid with mild stenosis through a porous medium in an endoscope. *Journal of Porous Media*, 22(9).
44. Hafez, N. M., Abd-Alla, A. M., & Metwaly, T. M. N. (2023). Influences of rotation and mass and heat transfer on MHD peristaltic transport of Casson fluid through inclined plane. *Alexandria Engineering Journal*, 68, 665-692.

45. Devakar, M., Ramesh, K., & Vajravelu, K. (2022). Magnetohydrodynamic effects on the peristaltic flow of couple stress fluid in an inclined tube with endoscope. *Journal of Computational Mathematics and Data Science*, 2, 100025.
46. Hayat, T., Tanveer, A., Yasmin, H., & Alsaedi, A. (2014). Effects of convective conditions and chemical reaction on peristaltic flow of Eyring-Powell fluid. *Applied Bionics and Biomechanics*, 11(4), 221-233.